NASA Contractor Report 198477

Nonlinear Spatial Evolution of Inviscid Instabilities on Hypersonic Boundary Layers

David W. Wundrow
NYMA, Inc.
Brook Park, Ohio

May 1996

Prepared for
Lewis Research Center
Under Contract NAS3–27186

National Aeronautics and
Space Administration

Nonlinear spatial evolution of inviscid instabilities on hypersonic boundary layers

By DAVID W. WUNDROW[1]

[1]Nyma, Inc., Lewis Research Center Group, Cleveland, Ohio 44135, USA

Abstract

The spatial development of an initially linear vorticity-mode instability on a compressible flat-plate boundary layer is considered. The analysis is done in the framework of the hypersonic limit where the free-stream Mach number $M \to \infty$. Nonlinearity is shown to become important locally, in a thin critical layer, when σ, the deviation of the phase speed from unity, becomes $o\left(M^{-\frac{8}{7}}\right)$ and the magnitude of the pressure fluctuations becomes $O\left(\sigma^{\frac{5}{2}}M^2\right)$. The unsteady flow outside the critical layer takes the form of a linear instability wave but with its amplitude completely determined by the nonlinear flow within the critical layer. The coupled set of equations which govern the critical-layer dynamics reflect a balance between spatial-evolution, (linear and nonlinear) convection and nonlinear vorticity-generation terms. The numerical solution to these equations shows that nonlinear effects produce a dramatic reduction in the instability-wave amplitude.

1. Introduction

The theory of compressible boundary-layer instabilities has received renewed attention in recent years primarily due to the current interest in hypersonic flight. The foundations of the linear theory were provided by Lees & Lin (1946) who showed that compressible boundary layers are often inviscidly unstable due to the presence of a generalized inflection point. Indeed, at sufficiently large Mach numbers, it is believed that laminar boundary-layer

instabilities are predominantly inviscid.

A comprehensive account of the linear inviscid stability theory is given by Mack (1984,1987). There it is shown that, in addition to the single inflectional mode present at all non-zero Mach numbers, the Rayleigh problem admits a countably infinite set of solutions whenever there is a region of supersonic flow relative to the phase speed of the disturbance. An example of this multiplicity of solutions is shown in figure 1 where the spatial growth rate $-\alpha_i$ is plotted against the frequency S for an insulated flat plate at a free-stream Mach number $M = 10$. In this figure, Mack's (1987) method of identifying families of eigensolutions associated with the neutral sonic modes is used. The first family, denoted Σ_u, starts from the upstream running Mach wave at $S = 0$ where $c = 1 - 1/M$ while the other families, denoted Σ_{dn}, start from the successive downstream running Mach waves at $S = S_{dn}$ where $c = 1 + 1/M$. Only solutions for $c_r \leqslant 1$ are presented in the figure so the Σ_{dn} curves begin at the frequencies S_{1n} corresponding to the non-inflectional neutral points with $c = 1$. The Σ_{dn} curves are shown only for a small range of S, were this range extended, the damping rate along each curve would, in general, reach a maximum and then decrease toward zero. The other neutral frequencies shown in figure 1 are denoted by S_{sn} and correspond to the generalized inflection point. In this paper, the convention of referring to the Σ_u family as the vorticity mode and the Σ_{dn} families as the acoustic modes (with the first acoustic mode corresponding to Σ_{d1}, the second to Σ_{d2} and so on) will be followed.

Single-frequency excitation of compressible boundary layers gives rise to spatially growing instability waves. For excitation amplitudes and Reynolds numbers sufficiently small and large respectively, the initial evolution of such disturbances can be described by weakly nonparallel linear stability theory. According to this theory, the instability wave continues

to grow as it propagates downstream and, owing to the growth of the mean boundary layer, the local Strouhal number increases. The latter result follows from the definition of the local Strouhal number as $\delta F^*/U_\infty$ where δ is a measure of the local boundary-layer thickness, F^* is the constant forcing angular frequency and U_∞ is the constant free-stream velocity. For simplicity, the mean flows considered here are assumed to be self-similar so the local stability properties can be found from eigenvalue diagrams such as figure 1 where S is now interpreted as the local Strouhal number.

As the local Strouhal number increases towards its neutral value, nonlinearity will come into play locally, in a thin critical layer, to balance the resulting singularity in the Rayleigh equation provided the Reynolds number is sufficiently large (see Goldstein & Leib 1988). This nonlinear interaction can be described by an analysis completely parallel to that given, for compressible shear layers, by Goldstein & Leib (1989) and Leib (1991). For the shear layers, the near-neutral region is the first region in which nonlinearity enters the development of the unsteady flow provided the instability-wave amplitude remains small. However, for the boundary layers of interest here, nonlinearity can become important away from the near-neutral region while disturbance is still small due to the interplay between the vorticity and acoustic modes. This was first noted in the large Mach number analysis of the Rayleigh problem done by Blackaby, Cowley & Hall (1992, hereinafter referred to as BCH). They show that near each non-inflectional neutral frequency S_{1n} the vorticity mode has a well-defined critical layer and consequently, may be preferentially affected by nonlinearity. Referring to figure 1, this means that if a vorticity mode, with a dimensionless frequency 0.1 say, is excited, nonlinearity can become important as the local Strouhal number approaches either S_{12} or S_{13} (far from the neutral Strouhal number S_{s4}) while the instability-wave amplitude

is still small. It is this possibility that will be investigated in the present work.

As in the compressible-shear-flow analysis of Goldstein & Leib (1989) and Leib (1991) and the incompressible boundary and shear layer analyses of Goldstein Durbin & Leib (1987), Goldstein & Leib (1988) and Goldstein & Hultgren (1988), nonlinearity comes into play locally, in a thin critical layer, to balance a singularity in the Rayleigh equation only now the singularity arises as the local Strouhal number approaches a non-inflectional neutral value. The unsteady flow outside the critical layer remains essentially linear but with a slowly varying amplitude that is completely determined by the nonlinear dynamics in the critical layer. The appropriate scaling between the local instability-wave amplitude and frequency for which this nonlinear interaction takes place is determined by requiring that the nonlinear problem match onto the linear small-growth-rate solution far upstream. This ensures that the nonlinear solution represents the natural downstream continuation of the upstream linear solution.

To obtain a description of this nonlinear interaction from a first principles analysis, it is necessary to characterize, in some rational way, the relative sizes of the linear growth rate and wavenumber. This characterization is most easily arrived at by considering the problem in the hypersonic limit where the free-stream Mach number $M \to \infty$. The relevant asymptotic solutions to the Rayleigh problem, for a fluid obeying Chapman's viscosity law, are then given by Cowley & Hall (1990) and Smith & Brown (1990). The former reference contains an analysis of the small-wavenumber acoustic modes while the latter gives order-one wavenumber solutions for the vorticity mode as well as the acoustic modes. A detailed analysis of both mode types is given by BCH for a fluid satisfying the more accurate Sutherland viscosity law and Grubin & Trigub (1992a,b) present solutions for a fluid with a Prandtl number less than

unity and a power law viscosity-temperature relation.

The nonlinear interaction considered here is inherently a large Mach number phenomenon because it requires that the first few S_{1n} lie within the frequency range of the unstable vorticity mode (c.f. figure 3). But, from a practical stand point, the Mach number should not be too large since as it increases the frequency of the most rapidly growing vorticity-mode solution (and consequently, the excitation frequency of most interest) moves beyond the range in which the interplay with the merged acoustic modes produces a well-defined critical layer (see BCH). For an insulated flat plate, these considerations restrict the Mach number to values between about 8 and 20 which, nevertheless, is a range of technological interest. BCH indicate that their asymptotic solution for the vorticity mode is not in overall agreement with the exact solution until $M > 20$. It is felt that the nonlinear evolution equations to be derived here will remain valid in the more moderate range, $8 < M < 20$, for the following reasons. The present analysis involves only the linear solutions for the vorticity mode near the non-inflectional neutral frequencies S_{1n} and these solutions are in, at least, qualitative agreement with the exact solutions at lower Mach numbers. Also, the nonlinear interaction is local in nature and, to a large extent, its occurrence depends only on the requirement that the linear growth rate be small compared to the wavenumber which is certainly the case in the Mach number range of interest.

Goldstein & Wundrow (1990) showed that the aforementioned nonlinear mechanism causes a breakdown in the linear solution of Cowley & Hall (1990) when the amplitude of the pressure fluctuations in the main boundary layer becomes $O\left(M^{-4}\ln^{-1}M^2\right)$. Although presented in the context of acoustic modes, these analyses also apply to the vorticity mode

in the vicinity of the non-inflectional neutral frequencies[1]. The solutions to the nonlinear critical-layer problem derived in Goldstein & Wundrow (1990) depend on a single free parameter, r, which is defined as the ratio of the logarithmic derivative of the mean temperature to the logarithmic derivative of the mean vorticity evaluated at the transverse position where the phase speed of the disturbance equals the mean flow speed. This parameter is between 0 and 1 on the acoustic-mode branch of the linear solution and is greater than 1 on the vorticity-mode branch. The authors only presented numerical results for values of r less than 1, however these results clearly show the significance of nonlinear vorticity generation due to compressible effects. In particular, for values of r near 1 they found that these effects come into play first to produce a dramatic increase in the instability-wave growth rate.

The purpose of the present work is to determine how critical-layer nonlinearity affects the spatial development of an initially linear vorticity mode as it nears a non-inflectional neutral frequency. This objective could be achieved by computing solutions to the evolution equations derived in Goldstein & Wundrow (1990) for values of r greater than 1, however two changes will be made to the derivation of these equations which will greatly broaden their range of applicability. First, Sutherland's law will be used to model the variation of the viscosity with temperature instead of Chapman's law since, as pointed out by BCH, the former law is better suited for the large temperature variations encountered at hypersonic speeds; and second, the frequency range over which the nonlinear analysis applies will be enlarged to capture the maximum possible deviation from S_{1n} for which the linear vorticity

[1]The approximate linear dispersion relation obtained in Cowley & Hall (1990) and Goldstein & Wundrow (1990) has two branches for which the growth rate is positive. One branch corresponds to the amplified acoustic modes and the other corresponds to those amplified vorticity-mode solutions lying near the non-inflectional neutral frequencies S_{1n}. This issue is explored in some detail by BCH.

mode has a well-defined critical layer.

In the present analysis, nonlinearity first becomes important when the amplitude of the pressure fluctuations in the main part of the boundary layer becomes $O\left(\sigma^{\frac{5}{2}}M^2\right)$ where σ is a measure of the deviation of the local phase speed from unity and must be $o\left(M^{-\frac{8}{7}}\right)$. The coupled set of nonlinear equations that determine the critical-layer dynamics are a special case of those obtained by Goldstein & Wundrow (1990) and must be solved numerically. The computations show that, rather than enhancing the growth rate as it did in Goldstein & Wundrow (1990), nonlinearity now causes a dramatic reduction in the instability-wave amplitude - presumably because the nonlinear vorticity-generation (or Bjerknes) term appearing in the final critical-layer vorticity equation changes sign relative to the linear inhomogeneous term when solutions for the vorticity mode are considered.

The overall plan of the paper is as follows. The problem is formulated in §2, where the nonlinear flow is shown to gradually evolve from the strictly linear large M solution. The unsteady flow outside the critical layer is a linear inviscid perturbation about the hypersonic (i.e. $M \gg 1$), non-interactive, boundary-layer flow analyzed in BCH and the solution for this flow is worked out in §3. In §4, a comparison between the asymptotic and exact solutions to the linear dispersion relation is made. The asymptotic solutions obtained in §§2 and 3 are then used to formulate the relevant critical-layer problem in §5 and the numerical solution to this problem is presented and discussed in §6.

2. Formulation

As in Goldstein & Wundrow (1990), concern here is with a nearly-inviscid, compressible, boundary-layer flow of a perfect gas over a flat plate. The flow parameters in the free stream

are used as reference quantities and are generally denoted by the subscript ∞. The reference length δ_0 is taken to be some suitable boundary-layer thickness (e.g. momentum thickness) in the region where nonlinearity first becomes important. The steady flow is then characterized by the Mach number

$$M \equiv \frac{U_\infty}{a_\infty}, \tag{2.1}$$

and the Reynolds number

$$R \equiv \frac{1}{1+C}\frac{U_\infty \delta_0}{\nu_\infty}, \tag{2.2}$$

where $a_\infty = \sqrt{\gamma \Re T_\infty}$ is the speed of sound in the free stream, $C \approx 110.4/T_\infty$ is the Sutherland constant for air temperatures measured in degrees Kelvin, ν is the kinematic viscosity, γ is the isentropic exponent of the gas and $\Re$ is the gas constant. When numerical values are needed, γ is taken to be 1.4 and C is taken to be 0.5 which corresponds to a typical free-stream temperature in the upper atmosphere.

The Reynolds number is assumed to be large enough so that the unsteady motion is essentially inviscid and unaffected by mean boundary-layer growth over the length scale on which the nonlinear interaction takes place (see (5.13) for a more precise restriction). To the required level of approximation, the mean pressure is then constant and the local mean velocity and temperature are given by

$$\{u_0, v_0\} = \{f'(\eta), 0\}, \tag{2.3}$$

and

$$\theta_0 = T(\eta), \tag{2.4}$$

respectively, where η is the Dorodnitsyn-Howarth variable (Stewartson 1964) which is related

to the transverse coordinate y by

$$y = \int_0^\eta T(s)\mathrm{d}s. \tag{2.5}$$

The local mean velocity and temperature fields are, of course, dependent on the constitutive relations used to describe the fluid. The simplest fluid to consider from an analytic stand point is a perfect gas with a Prandtl number of unity and a viscosity-temperature relation given by Chapman's law since, in this case, the mean profiles can be expressed in terms of the Blasius function. However, the large Mach number behavior of both the steady and unsteady solutions can be significantly altered when more realistic models are used. The most dramatic modification results when the viscosity law is changed. If Sutherland's viscosity law is used the steady flow takes on a double-layer structure in the limit as $M \to \infty$ (Freeman & Lam 1959) and BCH show that the asymptotic solutions to the Rayleigh problem proceed in inverse powers of M rather than $\sqrt{\ln M}$ as in the case of a Chapman-law fluid. A similar result is found by Grubin & Trigub (1992a,b) when the viscosity-temperature relation is given by a power law. The next most significant change occurs when Prandtl numbers other than unity are considered. This was investigated by Fu, Hall & Blackaby (1990) as well as Grubin & Trigub (1992a,b) and both show that the scaling of the mean flow remains unaltered but that the powers of M in the resulting asymptotic expansions depend on the Prandtl number. Finally, Fu, Hall & Blackaby (1990) considered the effects of gas dissociation and found that, despite modifying the quantitative results, these effects leave the qualitative results (i.e. the Mach number scalings and exponents) unaltered.

As previously stated, the fluid in the present investigation is taken to be a perfect gas with a viscosity given by Sutherland's law. It is now further assumed that the Prandtl number is unity. This yields a model that captures the essential large Mach number behavior needed

to formulate the nonlinear problem without resulting in an excessive amount of algebra. Accordingly, the function f in (2.3) is determined by

$$ff'' + 2\left(\frac{T^{\frac{1}{2}}}{T+C}f''\right)' = 0 \tag{2.6}$$

subject to the boundary conditions

$$f(0) = f'(0) = 0, \quad f'(\infty) = 1, \tag{2.7}$$

and the local mean temperature is expressed as

$$T = T_b + (1 - T_b)f' + \frac{\gamma - 1}{2}M^2(T_b + f')(1 - f') \tag{2.8}$$

with $T_b = 1$ for an insulated wall.

Freeman & Lam (1959) found that in the hypersonic limit the solution for f takes on a double-layer structure consisting of a wall layer where

$$\xi \equiv M^{\frac{1}{2}}\eta \tag{2.9}$$

is order one and a temperature adjustment layer where η is order one. In the wall layer, f expands like

$$f = M^{-\frac{1}{2}}f_0(\xi) + \cdots. \tag{2.10}$$

Substituting (2.9) and (2.10) into (2.6)-(2.8) and equating like powers of M, one obtains at leading order

$$f_0 f_0'' + 2\left(\frac{f_0''}{\sqrt{T_0}}\right)' = 0 \tag{2.11}$$

with

$$f_0(0) = f_0'(0) = 0, \quad f_0 = \xi + \xi_\infty + \frac{b}{3(\xi + \xi_\infty)^3} + \cdots \quad \text{as} \quad \xi \to \infty \tag{2.12}$$

where

$$T_0 \equiv \frac{\gamma - 1}{2} (T_b + f_0') (1 - f_0'), \tag{2.13}$$

$$b \equiv \frac{72}{(\gamma - 1)(T_b + 1)}, \tag{2.14}$$

and ξ_∞ is a constant which must be determined numerically. The temperature in the wall layer is $O(M^2)$ so it follows from (2.5) and (2.9) that this region has a thickness of $O(M^{\frac{3}{2}})$ in the physical coordinate y.

The algebraic approach to the free-stream conditions exhibited in the wall layer becomes exponential in the temperature adjustment layer where

$$f = \eta + M^{-\frac{1}{2}} \xi_\infty + M^{-2} g_2(\eta) + \cdots. \tag{2.15}$$

Substituting (2.15) into (2.6)-(2.8), g_2' is found to satisfy

$$\eta g_2'' + 2 \left(\frac{\sqrt{1 - \frac{1}{2}(\gamma - 1)(T_b + 1) g_2'}}{1 - \frac{1}{2}(\gamma - 1)(T_b + 1) g_2' + C} g_2'' \right)' = 0 \tag{2.16}$$

subject to

$$g_2' = -\frac{b}{\eta^4} + \cdots \quad \text{as} \quad \eta \to 0, \quad g_2' \to 0 \quad \text{as} \quad \eta \to \infty. \tag{2.17}$$

Since the temperature here is $O(1)$, the width of this region in terms of y is also $O(1)$. Therefore, in physical coordinates, the wall layer makes up the main part of the boundary layer with the temperature adjustment layer serving as a relatively thin region through which matching with the free stream is accomplished.

The unsteady motion is assumed to start as a linear, inviscid, spatially growing wave upstream in the flow. It is further supposed that the wave is monochromatic (at least initially) and two-dimensional since, in the Mach number range of interest, the most rapidly growing linear waves are planar (Mack 1984,1987). The nonlinear interaction to be considered here

occurs as the local Strouhal number approaches a non-inflectional neutral value S_{1n}. Non-linearity then affects the evolution of the unsteady flow over a streamwise scale that is long compared to the wavelength of the disturbance but short compared to the scale on which the mean flow develops. For the purposes of the present analysis, S can then be taken as a constant and given by

$$S \equiv \frac{\delta_0 F^*}{U_\infty} = S_{1n} + \sigma^2 M^{\frac{1}{2}} \bar{S}_1 \quad \text{as} \quad M \to \infty \tag{2.18}$$

where S_{1n} has an expansion in inverse powers of M, $\bar{S}_1$ is an order-one constant and $\sigma^2 M^{\frac{1}{2}} \ll 1$. The behaviors of the local phase speed c and complex wavenumber α depend on both the sign of $\bar{S}_1$ and the size of the small parameter σ. For flow over a flat plate at zero angle of attack, the local boundary-layer thickness and consequently, the local Strouhal number both increase monotonically with increasing downstream distance. The local Strouhal number then approaches S_{1n} from below so, in the streamwise region of interest, $\bar{S}_1$ is negative. The size of σ is chosen so that the linear wave has a well-defined critical layer. The analysis of BCH shows that this condition is satisfied if

$$M^{-2} \ll \sigma \ll M^{-\frac{8}{7}} \tag{2.19}$$

in which case

$$c = 1 - \sigma \bar{c}_1 + \cdots, \tag{2.20}$$

$$\mathrm{Re}\,\alpha = M^{-\frac{3}{2}} \bar{\alpha}_0 + \cdots, \tag{2.21}$$

and

$$\mathrm{Im}\,\alpha = -\sigma^{\frac{11}{4}} M^{\frac{1}{2}} \kappa_r + \cdots, \tag{2.22}$$

as $M \to \infty$, where $\bar{c}_1$, $\bar{\alpha}_0$ and κ_r are all order-one real constants. It should be noted that the so-called acoustic-mode scaling, on which the analysis of Goldstein & Wundrow (1990) is

based, is recovered, for the present choice of viscosity law, when $\sigma = M^{-2}$. The analysis to follow, however, does not apply to this scaling and a separate treatment would be necessary to capture this smaller range of frequency deviations.

The critical layer is centered about the transverse position where the phase speed of the disturbance equals the mean flow speed. From (2.3) and (2.20), this requires $f' - 1 = O(\sigma)$ which, in view of (2.15), (2.17) and (2.19), is satisfied in an overlap region between the wall and temperature adjustment layers where

$$z \equiv \sigma^{\frac{1}{4}} M^{\frac{1}{2}} \eta \tag{2.23}$$

is order one. The flow will be nonlinear in this layer provided the local instability-wave amplitude is sufficiently large.

The unsteady flow remains predominantly linear outside the critical layer so the relevant solutions for the streamwise and transverse components of velocity, the temperature and the pressure expand like

$$u = f' + \epsilon \mathrm{Re}\Psi_1 A^\dagger \mathrm{e}^{\mathrm{i}\bar{X}} + \epsilon^2 u_2 + \epsilon\sigma^{\frac{15}{4}} M^4 u_3 + \cdots, \tag{2.24}$$

$$v = -M^{-\frac{3}{2}} \epsilon \mathrm{Re}\mathrm{i}\bar{\alpha}\Phi_1 A^\dagger \mathrm{e}^{\mathrm{i}\bar{X}} + \epsilon^2 v_2 + \epsilon\sigma^{\frac{15}{4}} M^4 v_3 + \cdots, \tag{2.25}$$

$$\theta = T + \epsilon \mathrm{Re}\Theta_1 A^\dagger \mathrm{e}^{\mathrm{i}\bar{X}} + \epsilon^2 \theta_2 + \epsilon\sigma^{\frac{15}{4}} M^4 \theta_3 + \cdots, \tag{2.26}$$

and

$$p^{\frac{1}{\gamma}} = 1 + \epsilon \mathrm{Re}\Pi_1 A^\dagger \mathrm{e}^{\mathrm{i}\bar{X}} + \epsilon^2 \pi_2 + \epsilon\sigma^{\frac{15}{4}} M^4 \pi_3 + \cdots, \tag{2.27}$$

respectively, where

$$\bar{X} \equiv M^{-\frac{3}{2}} \bar{\alpha} [x - (1 - \sigma\bar{c})\, t] \tag{2.28}$$

denotes the streamwise coordinate in a reference frame moving with the wave and $\epsilon \ll 1$ is a characteristic amplitude of the instability wave in the region where nonlinearity first comes into play. This nonlinearity alters the solution over a streamwise scale inversely proportional to the local linear growth rate and is accounted for by the function $A^\dagger(x_1)$ where

$$x_1 \equiv \sigma^{\frac{11}{4}} M^{\frac{1}{2}} x. \tag{2.29}$$

The $O(\epsilon^2)$ terms in the above expansions account for higher-order corrections due to nonlinearity outside the critical layer while the $O(\epsilon\sigma^{\frac{15}{4}} M^4)$ terms are introduced to allow matching with the higher harmonics generated within the critical layer.

The relationship between ϵ, σ and M is determined by requiring that the lowest-order nonlinear terms appearing in the critical-layer vorticity equation are of the same order as the linear convection and non-equilibrium terms. This choice ensures that the nonlinear problem will reduce to the appropriate linear solution far upstream. The function $A^\dagger(x_1)$ will ultimately be determined by the nonlinear dynamics in the critical layer but matching with the upstream linear solution requires

$$A^\dagger \to a^\dagger e^{(\kappa_r + i\kappa_i)x_1} \quad \text{as} \quad x_1 \to -\infty \tag{2.30}$$

where $a^\dagger$ is a complex constant.

The local instability-wave amplitude ϵ is related to the amplitude of the imposed disturbance through the solution of the weakly nonparallel linear stability problem. For a given excitation amplitude, the ϵ-σ-M relation then determines the magnitude of the deviation of the local Strouhal number from S_{1n} in the streamwise region where nonlinearity is expected to become important. The success of the theory for any given excitation amplitude depends on how well (2.21) and (2.22) approximate the wavenumber in that region as determined

by the local compressible Rayleigh problem. A further constraint on the theory is given by (2.19) since this condition ultimately leads to a restriction on the size of ϵ (see (5.15) below) and consequently, on the excitation amplitude.

The functions Π_1, Φ_1, Ψ_1 and Θ_1 of η, x_1, σ and M are determined, to the required level of approximation, by

$$(f'-c)^2\frac{\partial}{\partial\eta}\left[\frac{1}{(f'-c)^2}\frac{\partial\Pi_1}{\partial\eta}\right]-\alpha^2T^2\left[1-M^2\frac{(f'-c)^2}{T}\right]\Pi_1=0, \tag{2.31}$$

$$\frac{\partial}{\partial\eta}\left(\frac{\Phi_1}{f'-c}\right)=-T\left[M^{-2}\frac{T}{(f'-c)^2}-1\right]\Pi_1, \tag{2.32}$$

$$\Psi_1=-M^{-2}\frac{T}{f'-c}\Pi_1+\frac{f''}{T(f'-c)}\Phi_1, \tag{2.33}$$

and

$$\Theta_1=(\gamma-1)T\Pi_1+\frac{T'}{T(f'-c)}\Phi_1, \tag{2.34}$$

subject to the boundary conditions

$$\frac{\partial\Pi_1}{\partial\eta}=0 \quad \text{at} \quad \eta=0, \quad \Pi_1\to 0 \quad \text{as} \quad \eta\to\infty, \tag{2.35}$$

where the complex wavenumber and phase speed are now given by

$$\alpha=M^{-\frac{3}{2}}\left(\bar{\alpha}+\sigma^{\frac{11}{4}}M^2\frac{1}{\mathrm{i}A^\dagger}\frac{\mathrm{d}A^\dagger}{\mathrm{d}x_1}\right), \tag{2.36}$$

and

$$c=1-\sigma\bar{c}-\sigma^{\frac{11}{4}}M^2\frac{1}{\mathrm{i}\bar{\alpha}A^\dagger}\frac{\mathrm{d}A^\dagger}{\mathrm{d}x_1}, \tag{2.37}$$

respectively, and the real constants $\bar{\alpha}$ and $\bar{c}$ have expansions of the form

$$\bar{\alpha}=\bar{\alpha}_0+\sigma^2M^2\bar{\alpha}_1+\cdots \tag{2.38}$$

and

$$\bar{c}=\bar{c}_1+\cdots. \tag{2.39}$$

It should be noted that the next correction to the mean flow in the wall layer was found by BCH to produce an $O\left(M^{-\frac{1}{2}(1+\sqrt{7})}\right)$ term in (2.38). Although the essential results for the linear flow outside the critical layer are unaltered by this term, (2.19) is stiffened slightly by requiring

$$\sigma \gg M^{-\frac{1}{4}(5+\sqrt{7})} \tag{2.40}$$

so as to keep the linear analysis as straight-forward as possible.

In the next section, approximations for Π_1, Φ_1, Ψ_1 and Θ_1 valid outside the critical layer are derived. To facilitate in this derivation, a schematic of the asymptotic structure of the flow field in the Dorodnitsyn-Howarth variable is given in figure 2.

3. Unsteady solution outside the critical layer

First, the unsteady solution in the wall layer where $\xi = O(1)$ is considered. In this region, Π_1 expands like

$$\Pi_1 = P_0 + \sigma^2 M^2 P_1 + \cdots + \mathrm{i}\sigma^{\frac{11}{4}} M^2 P_{\mathrm{i}} + \cdots \tag{3.1}$$

where, without loss of generality, P_0 is taken to be real so that $\mathrm{i}P_{\mathrm{i}}$ is the first imaginary term. Substituting this expansion, along with (2.9) and (2.10), into (2.8) and (2.31) and equating like powers of σ and M the following equations are obtained

$$\mathcal{L}P_0 = 0, \tag{3.2}$$

$$\mathcal{L}P_1 = 2\frac{\bar{\alpha}_1}{\bar{\alpha}_0}\left\{\bar{\alpha}_0^2 T_0^2\left[1 - \frac{(f_0'-1)^2}{T_0}\right]P_0\right\}, \tag{3.3}$$

and

$$\mathcal{L}P_{\mathrm{i}} = 2\mathrm{Im}\left(\frac{1}{\mathrm{i}\bar{\alpha}_0 A^\dagger}\frac{\mathrm{d}A^\dagger}{\mathrm{d}x_1}\right)\left\{\left(\frac{1}{f_0'-1}\right)' P_0' + \bar{\alpha}_0^2 T_0^2\left[1 - \frac{(f_0'-1)\,f_0'}{T_0}\right]P_0\right\}, \tag{3.4}$$

where

$$\mathcal{L} \equiv (f_0' - 1)^2 \frac{\partial}{\partial \xi}\left[\frac{1}{(f_0' - 1)^2}\frac{\partial}{\partial \xi}\right] - \bar{\alpha}_0^2 T_0^2 \left[1 - \frac{(f_0' - 1)^2}{T_0}\right]. \tag{3.5}$$

In the frequency range of interest, the eigenfunction is concentrated in the wall layer so, in addition to the usual wall boundary conditions

$$P_0'(0) = P_1'(0) = P_i'(0) = 0, \tag{3.6}$$

the solutions to (3.2)-(3.4) must also satisfy

$$P_0 \sim -\frac{b^2}{7\xi^7} B_0, \quad P_1 \sim 2\frac{\bar{\alpha}_1}{\bar{\alpha}_0} B_0 C_1, \quad P_i \sim -2\mathrm{Im}\left(\frac{1}{\mathrm{i}\bar{\alpha}_0 A^\dagger}\frac{\mathrm{d}A^\dagger}{\mathrm{d}x_1}\right) B_0 C_i, \tag{3.7}$$

as $\xi \to \infty$, where B_0 is a nonzero constant which depends on the normalization chosen for Π_1 and the constants C_1 and C_i are found by the method of variation of parameters to be

$$C_1 = \frac{1}{B_0^2}\int_0^\infty \left(\frac{P_0'}{1 - f_0'}\right)^2 \mathrm{d}\xi, \tag{3.8}$$

and

$$C_i = \frac{1}{B_0^2}\int_0^\infty \left(\frac{1}{1 - f_0'}\right)^3 \left(f_0' P_0'^2 + \bar{\alpha}_0^2 T_0^2 P_0^2\right) \mathrm{d}\xi. \tag{3.9}$$

A numerical solution to (3.2) subject to (3.6) and (3.7) yields a countably infinite set of eigenvalues $\bar{\alpha}_0$ each of which corresponds to a non-inflectional neutral frequency S_{1n}.

The solution given by (3.1) breaks down in the overlap region where $z = O(1)$. The appropriate expansion, in this region, is

$$\Pi_1 = \sigma^2 M^2 E_0 + \cdots + \sigma^{\frac{7}{4}} \bar{P}_1 + \cdots + \mathrm{i}\sigma^{\frac{7}{2}} M^2 \bar{P}_i + \cdots \tag{3.10}$$

where E_0 is a real constant and $\bar{P}_1$ and $\mathrm{i}\bar{P}_i$ contain the first non-constant real and imaginary terms respectively. It is easy to see from (2.9), (2.10), (2.12) and (2.23) that in this region

$$f' = 1 - \sigma\frac{b}{z^4} + \cdots. \tag{3.11}$$

Substituting (3.10) and (3.11), along with (2.23), into (2.8) and (2.31) one finds, after integrating twice with respect to z,

$$\bar{P}_1 = D_1\left(-\frac{b^2}{7z^7} + \frac{2b\bar{c}_1}{3z^3} + \bar{c}_1^2 z\right) + E_1, \tag{3.12}$$

and

$$\begin{aligned}\bar{P}_i = &-3^5\frac{\bar{\alpha}_0^2}{b^2}\left(\frac{b}{\bar{c}_1}\right)^{\frac{1}{4}} E_0\left(\mathrm{Im}\,\phi^{\pm} + D_i\right)\left(-\frac{b^2}{7z^7} + \frac{2b\bar{c}_1}{3z^3} + \bar{c}_1^2 z\right)\\ &+2\mathrm{Im}\left(\frac{1}{\mathrm{i}\bar{\alpha}_0 A^{\dagger}}\frac{\mathrm{d}A^{\dagger}}{\mathrm{d}x_1}\right) D_1\left(\frac{b}{3z^3} + \bar{c}_1 z\right) + E_i\end{aligned} \tag{3.13}$$

where D_1, E_1, D_i, E_i and $\phi^{\pm}$ are at most functions of x_1 (the latter of which can be different depending on whether $z \gtrless (b/\bar{c}_1)^{\frac{1}{4}}$).

The eigenfunction must be rescaled again in the temperature adjustment layer. The solution here turns out to be

$$\Pi_1 = \sigma^2 M^2 E_0 + \cdots + \sigma^2 M^{\frac{1}{2}}\left(F_1\eta + G_1\right) + \cdots + \mathrm{i}\sigma^{\frac{15}{4}} M^{\frac{5}{2}}\left(F_i\eta + G_i\right) + \cdots \tag{3.14}$$

where only the first terms containing non-constant real and imaginary parts are shown. Clearly, (3.14) does not satisfy the free-stream boundary condition given by (2.35) and it is, therefore, necessary to introduce an outer region where the variable

$$\zeta = M^{-\frac{3}{2}}\eta \tag{3.15}$$

is order one. The solution in this region is given, to the required order of accuracy, by

$$\Pi_1 \sim Q\exp\left(-\bar{\alpha}\sqrt{1-\sigma^2 M^2\bar{c}^2}\;\zeta\right) \tag{3.16}$$

where the constant Q has an expansion in powers of σ and M.

The solutions in the various regions must, of course, be matched. The relevant results of this process are

$$E_0 = 2\frac{\bar{\alpha}_1}{\bar{\alpha}_0} B_0 C_1, \tag{3.17}$$

$$D_1 = B_0, \tag{3.18}$$

$$D_i = -\mathrm{Im}\phi^-, \tag{3.19}$$

$$\bar{\alpha}_1 = -\frac{\bar{c}_1^2}{2C_1}, \tag{3.20}$$

and

$$\mathrm{Im}\left(\frac{1}{\mathrm{i}A^\dagger}\frac{\mathrm{d}A^\dagger}{\mathrm{d}x_1}\right) = -\frac{3^5}{2} b\bar{\alpha}_0^2 \left(\frac{\bar{c}_1}{b}\right)^{\frac{11}{4}} \mathrm{Im}\left(\phi^+ - \phi^-\right), \tag{3.21}$$

where the last two equations form the leading-order approximation to the linear dispersion relation. The phase shift $\phi^+ - \phi^-$ appearing in (3.21) is ultimately determined by the nonlinear dynamics inside the critical layer but matching with the upstream linear solution requires

$$\phi^+ - \phi^- \to \mathrm{i}\pi \quad \text{as} \quad x_1 \to -\infty. \tag{3.22}$$

In order to formulate the nonlinear problem in the critical layer, it is necessary to have the expansions for Φ_1, Ψ_1 and Θ_1 near the transverse position where the phase speed of the disturbance equals the mean flow speed. These are obtained by substituting (3.10)-(3.13) along with (2.23) into (2.32)-(2.34) and expanding about $z = z_c \equiv (b/\bar{c}_1)^{\frac{1}{4}}$. The resulting expressions are

$$\Phi_1 = -\sigma M^{\frac{3}{2}} \frac{4b}{z_c^5}(z - z_c)\frac{B_0}{\bar{\alpha}_0^2} - \sigma^{\frac{11}{4}} M^{\frac{7}{2}} \left(324\frac{\bar{\alpha}_0\bar{c}_1^2}{bz_c^3} + \frac{1}{\mathrm{i}\bar{\alpha}_0 A^\dagger}\frac{\mathrm{d}A^\dagger}{\mathrm{d}x_1}\right)\frac{B_0}{\bar{\alpha}_0^2} + \cdots, \tag{3.23}$$

$$\Psi_1 = -\sigma^{\frac{1}{4}} \frac{b}{9z_c^2}(2z_c - z)\frac{B}{\bar{\alpha}_0^2} - \sigma^2 M^2 \left[J_0 + \frac{27}{b}\left(\ln|z - z_c| + \phi^\pm - \phi^-\right)\right]\bar{c}_1^2\frac{B_0}{\bar{\alpha}_0} + \cdots, \tag{3.24}$$

and

$$\Theta_1 = \sigma^{\frac{1}{4}} M^2 \frac{4}{z_c} \frac{B_0}{\bar{\alpha}_0^2} + \cdots, \tag{3.25}$$

where the real constant B has an expansion of the form

$$B = B_0 + \cdots + o\left(\sigma^{\frac{7}{4}} M^2\right), \tag{3.26}$$

J_0 is an order-one real constant and the dots indicate that higher-order terms in $z - z_c$ as well as in σ and M have been omitted. It is interesting to note that the leading-order temperature fluctuation given by (3.25) is bounded in the critical layer. This result, which differs from the singular behavior obtained by Reshotko (1960), is due to the long wavelength approximation being employed here and is the primary reason the critical-layer dynamics turn out to be strongly nonlinear rather than weakly nonlinear as in the compressible-shear-flow analysis of Goldstein & Leib (1989) and Leib (1991).

4. Linear dispersion relation

Before proceeding to a formulation of the nonlinear problem, some results obtained from the linear analysis are discussed.

The local Strouhal number of the instability wave can be expressed as

$$S = \alpha c = M^{-\frac{3}{2}} \bar{\alpha}_0 + \sigma^2 M^{\frac{1}{2}} \bar{\alpha}_1 + \cdots, \tag{4.1}$$

so it follows from (2.18) that

$$S_{1n} = M^{-\frac{3}{2}} \bar{\alpha}_0 + o\left(\sigma^2 M^{\frac{1}{2}}\right), \tag{4.2}$$

and $\bar{S}_1 = \bar{\alpha}_1$. Values of (4.2) corresponding to the first six $\bar{\alpha}_0$ determined by solving (3.2) subject to (3.6) and (3.7) are shown as a function of M in figure 3 for an insulated plate.

Also shown are the exact values of S_{1n} determined by solving (2.31) subject to (2.35) with $c = 1$. This figure demonstrates that, even at supersonic Mach numbers, the leading-order hypersonic solution provides a good approximation to S_{1n}.

In addition to the S_{1n} curves, the exact inflectional neutral frequencies S_{sn} are shown in figure 3. These values of S correspond to $c = f'(\eta_s)$ where η_s is determined by the generalized inflection point criterion,

$$\frac{1}{T}\left(\frac{f''}{T^2}\right)' = 0 \quad \text{at} \quad \eta = \eta_s. \tag{4.3}$$

As first observed by Mack (1984,1987), each S_{sn} curve has a range of M for which $\mathrm{d}S/\mathrm{d}M > 0$ and the corresponding neutral mode is vortical in character. In general, the rising portions of the curves mark the high frequency neutral point of the vorticity mode while the declining portions mark that point for the acoustic modes (c.f. figure 1). Figure 3 suggests that the slope of the rising portions tends to zero as the Mach number increases in contrast to the behavior exhibited in figure 6(a) of Cowely & Hall (1990) which was computed for a Chapman-law fluid. Smith & Brown (1990) found that along the rising segments in the latter figure S is $O(\sqrt{\ln M})$ as $M \to \infty$ while, for the Sutherland-law fluid considered here, BCH show that S is $O(1)$.

A direct comparison with Mack's (1984,1987) work is difficult since he used a combination of viscosity laws and took the Prandtl number to be 0.71. Still, the neutral curves in figure 3 as well as the growth rate curves in figure 1 are in qualitative agreement with his results. The assumption of a Prandtl number of unity made here appears to yield solutions which reasonably approximate those computed with a more accurate value. However, it should be noted that Grubin & Trigub (1992b) found significant changes to occur in the Rayleigh solutions when the Prandtl number is sufficiently small.

Having demonstrated an agreement between the exact and asymptotic properties of the neutral solutions, the behavior of the amplified waves is now considered. The local complex wavenumber of the linear disturbance is given by

$$\alpha = M^{-\frac{3}{2}} \left[\left(\bar{\alpha}_0 + \sigma^2 M^2 \bar{\alpha}_1 + \cdots \right) + \mathrm{i} \left(-\sigma^{\frac{11}{4}} M^2 \kappa_r + \cdots \right) \right] \tag{4.4}$$

where it follows from (2.30) and (3.20)-(3.22) that

$$\kappa_r = 2^{\frac{3}{8}} \cdot 3^5 \pi \Lambda \left(-\bar{\alpha}_1 \right)^{\frac{11}{8}} \tag{4.5}$$

with

$$\Lambda \equiv \frac{\bar{\alpha}_0^2}{b^{\frac{7}{4}}} C_1^{\frac{11}{8}}. \tag{4.6}$$

Equations (2.14) and (3.8) show that b and C_1 are real and positive, consequently, (4.5) requires negative values of $\bar{\alpha}_1$ to yield real values of κ_r. When $\bar{\alpha}_1$ is positive, the growth rate was found by BCH to be $O(\sigma M^{-\frac{3}{2}})$ so it follows from (4.1) and (4.2) that a discontinuity in the expansion for $\mathrm{Im}\alpha$ arises as S passes through S_{1n}. BCH went on to show how this discontinuity is smoothed out by the solution for the acoustic-mode scaling $\sigma = M^{-2}$. This aspect of the problem need not be considered here however, since, as mentioned in §2, $\bar{S}_1$ $(= \bar{\alpha}_1)$ is strictly negative in the streamwise region of interest.

The variation of κ_r with non-inflectional neutral frequency and wall temperature is determined by Λ. This quantity is shown as a function of T_b in figure 4 for the first two values of $\bar{\alpha}_0$. The curves show that, for fixed values of T_b, $\bar{\alpha}_1$ and M, the growth rate of the vorticity mode near the first non-inflectional neutral frequency S_{11} is less than that near the second S_{12} which is in agreement with the results shown in figure 1. The asymptotic solution predicts that this trend of increasing growth rates is continued for the subsequent

S_{1n}, yet, in figure 1, the growth rate of the vorticity mode near S_{13} is clearly less than that near S_{12}. This discrepancy is due to the fact that at $M = 10$ the third acoustic mode has only just merged with the vorticity mode (c.f. figure 3). At $M = 20$, figure 6.2 of BCH shows that the growth rate near S_{13} becomes greater than that near S_{12} in accordance with the asymptotic solution. If the growth rate associated with a particular non-inflectional neutral frequency is considered, figure 4 shows a decrease with decreasing T_b. This result may seem to contradict the conclusion that wall cooling has a destabilizing effect on the Mack's so-called higher modes (Mack 1984). However, figure 9.13 of Mack (1984) clearly shows that while the magnitudes of the peaks in the vorticity-mode growth rate increase with decreasing wall temperature, the growth rate in the valleys actually decreases.

Despite this qualitative agreement, quantitative agreement between the exact and asymptotic growth rates is not achieved until the Mach number becomes very large. Quantitative agreement is, however, not crucial in the present investigation because the final nonlinear problem turns out to be entirely independent of κ_r. In fact, the nonlinear dynamics depend only on the σ-M scaling of the growth rate. To determine the accuracy of this scaling, the exact vorticity-mode growth rate is computed as a function of M for a fixed deviation from a non-inflectional neutral frequency, that is for

$$S = (1 - \lambda)S_{1n} \tag{4.7}$$

where $0 < \lambda \ll 1$ is a constant. The results of this computation are presented in figure 5 for the first two values of S_{1n}. The asymptote predicted by the hypersonic solution is also shown. This is determined by noting that (4.1), (4.2) and (4.7) imply

$$\bar{\alpha}_1 \sim -\sigma^{-2}M^{-2}\lambda\bar{\alpha}_0 \tag{4.8}$$

which, from (2.19) and (2.40), requires

$$M^{-\frac{1}{2}(1+\sqrt{7})} \ll \lambda \ll M^{-\frac{2}{7}}. \tag{4.9}$$

Substituting (4.8) into (4.5) and the result into (4.4) gives

$$\alpha_i \equiv \mathrm{Im}\,\alpha = O\left(M^{-\frac{9}{4}}\lambda^{\frac{11}{8}}\right) \tag{4.10}$$

and, since λ is held fixed along the computed curves,

$$\frac{M}{\alpha_i}\frac{\mathrm{d}\alpha_i}{\mathrm{d}M} \sim -\frac{9}{4}. \tag{4.11}$$

Although the comparisons shown in figure 5 are fairly good, it is felt that improvements could be obtained by adding higher-order corrections to (4.10). However, such terms do not enter into the critical-layer analysis and so are not pursued here.

5. The critical layer

Equation (3.24) shows that the solution in the overlap region becomes singular where $z = z_c$. The governing equations must therefore be rescaled to obtain a bounded solution in this region. The thickness of the small-growth-rate critical layer is of the order of the mean velocity times the growth rate divided by the mean velocity gradient times the real part of the wavenumber so it follows from (2.36) and (3.11) that the appropriately scaled transverse coordinate in this region is

$$Z \equiv \sigma^{-\frac{7}{4}}M^{-2}(z - z_c). \tag{5.1}$$

Equations (2.24)-(2.27), (3.10), (3.11), (3.23)-(3.25), (A 1)-(A 4), (A 13) and (A 15)-(A 17) along with (5.1) suggest that the flow in this region should expand like

$$u = 1 - \sigma\bar{c} + \sigma^{\frac{11}{4}}M^2\frac{4b}{z_c^5}Z - \sigma^{\frac{9}{2}}M^4\frac{10b}{z_c^6}Z^2 - \sigma^{\frac{1}{4}}\epsilon\frac{b}{9z_c}\frac{B_0}{\bar{\alpha}_0^2}\mathrm{Re}\,A^{\dagger}\mathrm{e}^{\mathrm{i}\bar{X}}$$

$$+ \text{ bounded } Z\text{−independent terms} + \sigma^2 M^2 \epsilon \bar{u}_1 + \cdots, \tag{5.2}$$

$$v = \sigma^{\frac{11}{4}} M^2 \epsilon \mathrm{Re}\left[\left(\frac{4b}{z_c^5} Z + \frac{324}{b z_c^3}\bar{\alpha}_0 \bar{c}_1^2 + \frac{1}{\mathrm{i}\bar{\alpha}_0 A^\dagger}\frac{\mathrm{d}A^\dagger}{\mathrm{d}x_1}\right.\right.$$
$$\left.\left. -\sigma^{-\frac{5}{2}} M^{-2} \epsilon \frac{b}{9 z_c}\frac{B_0}{\bar{\alpha}_0^2}\mathrm{Re}A^\dagger \mathrm{e}^{\mathrm{i}\bar{X}}\right)\frac{B_0}{\bar{\alpha}_0}\mathrm{i}A^\dagger \mathrm{e}^{\mathrm{i}\bar{X}}\right] + \cdots, \tag{5.3}$$

$$\theta = \sigma M^2 \frac{36}{z_c^4} - \sigma^{\frac{11}{4}} M^4 \frac{144}{z_c^5} Z + \sigma^{\frac{1}{4}} M^2 \epsilon \bar{\theta}_1 + \cdots, \tag{5.4}$$

and

$$p^{\frac{1}{\gamma}} = 1 - \sigma^2 M^2 \epsilon \frac{\bar{c}_1^2}{\bar{\alpha}_0} B_0 \mathrm{Re}A^\dagger \mathrm{e}^{\mathrm{i}\bar{X}} + \cdots. \tag{5.5}$$

This solution will match the 'outer' solution in the overlap region provided

$$\frac{\partial \bar{u}_1}{\partial Z} \to \frac{b}{9 z_c^2}\frac{B_0}{\bar{\alpha}_0^2}\mathrm{Re}A^\dagger \mathrm{e}^{\mathrm{i}\bar{X}}, \tag{5.6}$$

$$\bar{\theta}_1 \to \frac{4}{z_c}\frac{B_0}{\bar{\alpha}_0^2}\mathrm{Re}A^\dagger \mathrm{e}^{\mathrm{i}\bar{X}}, \tag{5.7}$$

as $Z \to \pm\infty$, and

$$\frac{1}{\pi}\int_0^{2\pi}\int_{-\infty}^{+\infty}\left(\frac{\partial \bar{u}_1}{\partial Z} - \frac{b}{9 z_c^2}\frac{B_0}{\bar{\alpha}_0^2}\mathrm{Re}A^\dagger \mathrm{e}^{\mathrm{i}\bar{X}}\right)\mathrm{e}^{-\mathrm{i}\bar{X}}\mathrm{d}Z\mathrm{d}\bar{X} = -\frac{27}{b}\frac{\bar{c}_1^2}{\bar{\alpha}_0} B_0 \left(\phi^+ - \phi^-\right) A^\dagger. \tag{5.8}$$

The functions $\bar{u}_1$ and $\bar{\theta}_1$ of $\bar{X}$, Z and x_1 are determined by the vorticity and energy equations which can be written as

$$\bar{D}\omega = \frac{\omega}{\gamma p}\bar{D}p + \sigma^{-\frac{3}{2}} M^{-\frac{7}{2}}\frac{1}{\gamma T p}\left[\left(\bar{\alpha}\frac{\partial p}{\partial \bar{X}} + \sigma^{\frac{11}{4}} M^2 \frac{\partial p}{\partial x_1}\right)\frac{\partial \theta}{\partial Z}\right.$$
$$\left. - \frac{\partial p}{\partial Z}\left(\bar{\alpha}\frac{\partial \theta}{\partial \bar{X}} + \sigma^{\frac{11}{4}} M^2 \frac{\partial \theta}{\partial x_1}\right)\right], \tag{5.9}$$

and

$$\bar{D}\theta = \frac{\gamma - 1}{\gamma}\frac{\theta}{p}\bar{D}p, \tag{5.10}$$

respectively, where

$$\bar{D} \equiv \sigma^{\frac{11}{4}} M^2 u \frac{\partial}{\partial x_1} + \bar{\alpha}(u - 1 + \sigma \bar{c})\frac{\partial}{\partial \bar{X}} + \sigma^{-\frac{3}{2}}\frac{v}{T}\frac{\partial}{\partial Z}, \tag{5.11}$$

$$\omega \equiv M^{-\frac{3}{2}}\left(\bar{\alpha}\frac{\partial v}{\partial \bar{X}} + \sigma^{\frac{11}{4}}M^2\frac{\partial v}{\partial x_1}\right) - \sigma^{-\frac{3}{2}}M^{-\frac{3}{2}}\frac{1}{T}\frac{\partial u}{\partial Z}, \tag{5.12}$$

and it has been assumed that

$$R \gg \sigma^{-\frac{21}{4}}M^{-\frac{5}{2}} \tag{5.13}$$

so, to the required level of approximation, terms accounting for viscous diffusion effects as well as those arising from corrections to the mean flow due to the growth of the boundary layer can be neglected.

The relationship between the amplitude scale ϵ, the phase speed deviation σ and the Mach number M is determined from (5.9)-(5.11) by requiring that the lowest-order velocity jump produced by the nonlinear terms is of the same order as the velocity jump due to linear effects, i.e. $O(\sigma^2 M^2 \epsilon)$. A little experimentation shows that nonlinear effects will influence $\bar{u}_1$ if

$$\epsilon = \sigma^{\frac{5}{2}}M^2 \tag{5.14}$$

which, when combined with (2.19) and (2.40), requires

$$M^{-\frac{1}{8}(9+5\sqrt{7})} \ll \epsilon \ll M^{-\frac{6}{7}}. \tag{5.15}$$

The equations governing $\bar{u}_1$ and $\bar{\theta}_1$ are then

$$\bar{\mathcal{D}}\left(\frac{\partial \bar{u}_1}{\partial Z} - \frac{4b}{z_c^6}Z\right) = \bar{c}_1^2 B_0 \mathrm{Re}\left(\mathrm{i}A^\dagger \mathrm{e}^{\mathrm{i}\bar{X}}\right)\frac{\partial}{\partial Z}\left(\bar{\theta}_1 - \frac{144}{z_c^5}Z\right) \tag{5.16}$$

and

$$\bar{\mathcal{D}}\left(\bar{\theta}_1 - \frac{144}{z_c^5}Z\right) = 0 \tag{5.17}$$

where

$$\begin{aligned}\bar{\mathcal{D}} \equiv \frac{\partial}{\partial x_1} + \bar{\alpha}_0\left(\frac{4b}{z_c^5}Z - \frac{b}{9z_c}\frac{B_0}{\bar{\alpha}_0^2}\mathrm{Re}A^\dagger \mathrm{e}^{\mathrm{i}\bar{X}}\right)\frac{\partial}{\partial \bar{X}} + \frac{z_c^4}{36}\frac{B_0}{\bar{\alpha}_0}\mathrm{Re}\left[\left(\frac{4b}{z_c^5}Z\right.\right. \\ \left.\left. + \frac{324}{bz_c^3}\bar{\alpha}_0\bar{c}_1^2 + \frac{1}{\mathrm{i}\bar{\alpha}_0 A^\dagger}\frac{\mathrm{d}A^\dagger}{\mathrm{d}x_1} - \frac{b}{9z_c}\frac{B_0}{\bar{\alpha}_0^2}\mathrm{Re}A^\dagger \mathrm{e}^{\mathrm{i}\bar{X}}\right)\mathrm{i}A^\dagger \mathrm{e}^{\mathrm{i}\bar{X}}\right]\frac{\partial}{\partial Z}\end{aligned} \tag{5.18}$$

is the limiting form of the total derivative in the critical layer.

The presence of $A^\dagger$ in the coefficients of both the $\partial_{\bar{X}}$ and ∂_Z terms in (5.18) as well as in the right-hand-side of (5.16) shows that nonlinearity enters the critical layer dynamics through both streamwise and transverse convection terms as well as through vorticity production due to pressure-density variations. The nonlinear streamwise convection terms turn out to be passive in that they do not affect the instability-wave growth rate (although they do strongly affect the flow field in the critical layer). These terms can be eliminated from (5.18) by simply introducing a strained transverse coordinate,

$$\bar{Z} \equiv Z - \frac{z_c^4}{36}\frac{B_0}{\bar{\alpha}_0^2}\mathrm{Re}\,A^\dagger \mathrm{e}^{\mathrm{i}\bar{X}} \tag{5.19}$$

so that $\bar{\mathcal{D}}$ becomes

$$\bar{\mathcal{D}} = \frac{\partial}{\partial x_1} + \frac{4b}{z_c^5}\bar{\alpha}_0\bar{Z}\frac{\partial}{\partial \bar{X}} + \frac{9z_c}{b}\bar{\alpha}_0\bar{c}_1 B_0 \mathrm{Re}\left(\mathrm{i}A^\dagger \mathrm{e}^{\mathrm{i}\bar{X}}\right)\frac{\partial}{\partial \bar{Z}}. \tag{5.20}$$

The parameters characterizing the 'outer' linear flow can be removed from the critical-layer equations by introducing the following normalized variables,

$$A \equiv -\frac{2^4}{3^8}\frac{z_c^{10}}{\bar{\alpha}_0^3}B_0 A^\dagger \mathrm{e}^{\mathrm{i}(X_0 - \kappa_i x_1)}, \tag{5.21}$$

$$\Omega \equiv -\frac{2}{3^5}\frac{z_c^{12}}{b\bar{\alpha}_0}\left(\frac{\partial \bar{u}_1}{\partial \bar{Z}} - \frac{b}{9z_c^2}\frac{B_0}{\bar{\alpha}_0^2}\mathrm{Re}A^\dagger \mathrm{e}^{\mathrm{i}\bar{X}}\right), \tag{5.22}$$

$$H \equiv \frac{1}{2\cdot 3^7}\frac{z_c^{11}}{\bar{\alpha}_0}\left(\bar{\theta}_1 - \frac{4}{z_c}\frac{B_0}{\bar{\alpha}_0^2}\mathrm{Re}A^\dagger \mathrm{e}^{\mathrm{i}\bar{X}}\right), \tag{5.23}$$

$$\bar{x} \equiv \frac{3^5}{2}\frac{b}{z_c^{11}}\bar{\alpha}_0^2 x_1 - \bar{x}_0, \tag{5.24}$$

$$X \equiv \bar{X} - X_0 + \kappa_i x_1, \tag{5.25}$$

and

$$Y \equiv \frac{2^3}{3^5}\frac{z_c^6}{\bar{\alpha}_0}\left(\bar{Z} + \frac{z_c^5}{4b}\frac{\kappa_i}{\bar{\alpha}_0}\right). \tag{5.26}$$

Equations (5.16), (5.17), (5.8) and (3.21) then become

$$\mathcal{D}\Omega = \mathrm{Re}\left(\mathrm{i}A\mathrm{e}^{\mathrm{i}X}\right)\left(4\frac{\partial H}{\partial Y} - 3\right), \tag{5.27}$$

$$\mathcal{D}H = -\mathrm{Re}\left(\mathrm{i}A\mathrm{e}^{\mathrm{i}X}\right), \tag{5.28}$$

$$\frac{1}{\pi}\int_0^{2\pi}\int_{-\infty}^{+\infty}\Omega\mathrm{e}^{-\mathrm{i}X}\mathrm{d}Y\,\mathrm{d}X = -3(\phi^+ - \phi^-)A, \tag{5.29}$$

and

$$\mathrm{Im}(\phi^+ - \phi^-) = -\mathrm{Im}\left(\frac{1}{\mathrm{i}A}\frac{\mathrm{d}A}{\mathrm{d}\bar{x}}\right), \tag{5.30}$$

respectively, where

$$\mathcal{D} \equiv \frac{\partial}{\partial\bar{x}} + Y\frac{\partial}{\partial X} - \mathrm{Re}\left(\mathrm{i}A\mathrm{e}^{\mathrm{i}X}\right)\frac{\partial}{\partial Y}. \tag{5.31}$$

If the, as yet, unspecified real constants X_0 and $\bar{x}_0$ are chosen to be

$$X_0 = -\arg\left(-B_0 a^\dagger\right), \tag{5.32}$$

and

$$x_0 = -\frac{1}{\pi}\ln\left(\frac{2^4}{3^8}\frac{z_c^{10}}{\bar{\alpha}_0^3}|B_0 a^\dagger|\right), \tag{5.33}$$

(2.30) becomes

$$A \to \mathrm{e}^{\pi\bar{x}} \quad \text{as} \quad \bar{x} \to -\infty. \tag{5.34}$$

From this condition along with (3.22) and (5.27)-(5.29), one can show that the solution for A remains real for all values of $\bar{x}$. Equations (5.29) and (5.30) can then be combined to give

$$\frac{1}{\pi}\int_0^{2\pi}\int_{-\infty}^{+\infty}\Omega\mathrm{e}^{-\mathrm{i}X}\mathrm{d}Y\,\mathrm{d}X = -\mathrm{i}3\frac{\mathrm{d}A}{\mathrm{d}\bar{x}}. \tag{5.35}$$

It should be noted that equations (5.27) and (5.28) are the same as equations (6.29) and (6.30) of Goldstein & Wundrow (1990) but with $r = 4$. The difference in the velocity jump

condition given by (5.35) and that given by equation (6.31) of Goldstein & Wundrow (1990) with $r = 4$ is due to a difference in normalizations which can be eliminated by replacing their Γ with $(1 - r)\Gamma$ in equations (6.22)-(6.27) of the latter analysis.

Equations (5.27), (5.28) and (5.35) must be solved numerically subject to matching with both the 'outer' flow in the overlap region and the linear flow upstream. The former condition requires that Ω and H be strictly periodic in X and satisfy the homogeneous boundary conditions

$$\Omega,\ H \to 0 \quad \text{as} \quad Y \to \pm\infty, \tag{5.36}$$

while the latter, in addition to (5.34), requires

$$\Omega \to -3\mathrm{Re}\left(\frac{1}{Y - \mathrm{i}\pi} A\mathrm{e}^{\mathrm{i}X}\right) \tag{5.37}$$

and

$$H \to -\mathrm{Re}\left(\frac{1}{Y - \mathrm{i}\pi} A\mathrm{e}^{\mathrm{i}X}\right), \tag{5.38}$$

as $\bar{x} \to -\infty$. The technique used to solve the final critical-layer problem parallels that given in Goldstein & Wundrow (1990) and the reader is referred there for a detailed discussion of the method.

6. Numerical results and discussion

Goldstein & Wundrow (1990) considered the spatial development of an initially linear inviscid instability wave on a hypersonic boundary layer. Their analysis was done for a fluid satisfying Chapman's viscosity law using the acoustic-mode scaling which, in the present analysis, corresponds to $\sigma = M^{-2}$. The evolution equations they derived depend on a single free parameter, r, which is defined as the ratio of the logarithmic derivative of the mean

temperature to the logarithmic derivative of the mean vorticity evaluated at the critical level. For the amplified acoustic modes, r varies between 0 at the non-inflectional neutral frequency S_{1n} and 1 at the inflectional neutral frequency S_{sn}. For the amplified vorticity mode, r must be greater than some minimum value which is determined by the asymptotic solution to the Rayleigh problem and is itself greater than 1. This condition reflects the fact that the phase speeds of the vorticity-mode solutions to which the nonlinear theory applies are less than those of the amplified acoustic modes and so the critical layer is located closer to the wall where the mean temperature variations out weigh the mean vorticity variations.

Goldstein & Wundrow (1990) only presented numerical results for the case when the disturbance is an acoustic mode, i.e. for $r < 1$. These results show that nonlinear vorticity generation in the critical layer can cause a super-exponential growth of the instability wave but that this subsides once the wave amplitude becomes sufficiently large. Transverse convection effects then come into play to produce a nonlinear roll-up of the flow within the critical layer and this, in turn, drives the growth rate toward zero. The final asymptotic state of the critical layer, for $r < 1$, is left undetermined but the authors indicate that viscous effects will eventually become important due to the continually decreasing scales generated by the roll-up. The incompressible-shear-flow analysis of Goldstein & Hultgren (1988) along with the investigation of the upper-branch stability of compressible boundary layers due to Gajjar & Cole (1989) suggest that viscous effects will ultimately produce a quasi-equilibrium critical-layer structure and a slow algebraic growth of the instability wave.

Of primary interest, in the present investigation, is how the numerical results given in Goldstein & Wundrow (1990) are altered when $r = 4$, i.e. for the case of more practical importance when the disturbance is a vorticity mode. In figure 6, the scaled instability-

wave amplitude A determined by (5.27), (5.28) and (5.35) is shown as a function of the long streamwise variable $\bar{x}$. The corresponding instability-wave growth rate is presented in figure 7. These curves show that the wave grows linearly until its amplitude becomes large enough for nonlinear effects to become important. The growth rate then decreases and soon becomes negative. This results in a rapid reduction in the wave amplitude which is in contrast to the initial nonlinear amplification observed by Goldstein & Wundrow (1990). Both behaviors are the consequence of vorticity generation due to compressible effects. The difference presumably results because the nonlinear vorticity-generation (or Bjerknes) term appearing in the final critical-layer vorticity equation changes sign relative to the linear inhomogeneous term when r is greater than 1 (see equation (6.29) of Goldstein & Wundrow (1990)). The results presented in figures 5 and 6 correspond more closely to the special case found in the analysis of the weakly-nonlinear critical layer associated with a three-dimensional disturbance on a compressible shear layer done by Goldstein & Leib (1989) and Leib (1991). For this special case, the scaled amplitude function is purely real and figures 4 and 7 of the former analysis and figure 1 of the latter show that nonlinearity produces a rapid reduction in both the growth rate and wave amplitude.

Although the nonlinear terms in the critical-layer problem become less important as the instability-wave amplitude continues to decrease, the solution does not return to its upstream linear state. This is because the effects of the nonlinear redistribution of vorticity, which takes place near the peak in the amplitude, persist downstream in such a way that the growth rate remains negative. This redistribution is demonstrated in figure 8 where constant-vorticity lines in the $(X, \bar{Y})$ plane are shown at various values of $\bar{x}$. As in Goldstein & Wundrow (1990), localized regions of high vorticity are produced by the nonlinear coupling of the vorticity and

energy equations (c.f. figure 8(b)) while the more usual roll-up of the contours is the result of transverse convection effects (c.f. figure 8(c)). Superposed on this behavior is a straining of the contours due to the nonlinear streamwise convection term which has been re-introduced by showing the vorticity as a function of the more physical transverse coordinate,

$$\bar{Y} \equiv \frac{2^3}{3^5}\frac{z_c^6}{\bar{\alpha}_0}\left(Z + \frac{z_c^5}{4b}\frac{\kappa_i}{\bar{\alpha}_0}\right) = Y - \frac{3}{8}\mathrm{Re}\,A\mathrm{e}^{\mathrm{i}X}. \tag{6.1}$$

The straining is most pronounced in figure 8(c) where A is the largest. The important point to note is that, once the redistribution takes place, the vorticity field remains rolled-up even after the instability-wave amplitude has become quite small (c.f. figure 8(d)).

The results in figures 6 and 7 suggest that the quasi-equilibrium critical-layer structure proposed for the downstream behavior of the acoustic modes will not apply to the vorticity mode considered here. In fact, the numerical solution to the critical-layer problem predicts that the scaled amplitude of the vorticity mode goes to zero at a finite downstream distance. Before this point is reached, however, the asymptotic formulation outside the critical layer breaks down. To show this, the amplitudes of the higher harmonics generated within the critical layer must be determined. The equation governing these amplitudes is obtained by equating the expression for the velocity jump across the critical layer given by the 'outer' solution in the overlap region, (B 15), with that given by the 'inner' critical-layer solution and is expressed as

$$a_3^{(m)} \equiv \frac{2^4}{3^{12}}\frac{z_c^{17}}{m\bar{\alpha}_0^3\bar{c}_1^2}\mathrm{e}^{\mathrm{i}m(X_0-\kappa_i x_1)}\hat{a}_3^{(m)} = -\frac{1}{\pi}\int_0^{2\pi}\int_{-\infty}^{+\infty}\Omega\mathrm{e}^{\mathrm{i}mX}\mathrm{d}Y\mathrm{d}X \tag{6.2}$$

where $m = 2, 3, \ldots$. The amplitudes of the first few harmonics are shown in figure 9. It is clear that, as the amplitude of the fundamental goes to zero, the amplitudes of the higher harmonics do not. Consequently, the expansions (2.24)-(2.27) eventually become disordered.

A solution for the next stage of evolution is not worked out here because, once the amplitude of the fundamental becomes sufficiently small, other disturbances not accounted for by the present theory but always present in practice would then, most likely, be dominant.

Finally, viscous effects could be incorporated into the critical-layer analysis by loosening the restriction in (5.13). Some care must be taken in doing this, however, since it is possible that an interaction between the mean flow and the leading-edge shock of the sort considered by Bush & Cross (1967) could take place for certain values of σ. In any event, it is felt that, although viscosity will tend to reduce the gradients in the vorticity and temperature fields, it will not significantly alter the behavior of the instability-wave amplitude because the nonlinear interaction that drives the amplitude to zero occurs over such a short distance (on the $\bar{x}$ scale) that viscous effects would not have time to assert themselves.

Appendix A. Nonlinear terms in the overlap region

The lowest-order approximations (in σ, M and $z-z_c$) of the $O(\epsilon^2)$ terms in the expansions (2.24)-(2.27) are determined in this appendix. Since these terms are generated by nonlinear interactions that are quadratic in the fundamental mode, they can be expressed as

$$u_2 + \pi_1 u_1 = \Psi_2^{(0)} + \mathrm{Re}\Psi_2^{(2)} \mathrm{e}^{\mathrm{i}2\bar{X}}, \tag{A 1}$$

$$v_2 + \pi_1 v_1 = -M^{-\frac{3}{2}} 2\bar{\alpha} \left(\Phi_2^{(0)} + \mathrm{Re}\mathrm{i}\Phi_2^{(2)} \mathrm{e}^{\mathrm{i}2\bar{X}} \right), \tag{A 2}$$

$$\theta_2 + \pi_1 \theta_1 = \Theta_2^{(0)} + \mathrm{Re}\Theta_2^{(2)} \mathrm{e}^{\mathrm{i}2\bar{X}}, \tag{A 3}$$

$$\pi_2 = \Pi_2^{(0)} + \mathrm{Re}\Pi_2^{(2)} \mathrm{e}^{\mathrm{i}2\bar{X}}, \tag{A 4}$$

where u_1, v_1, θ_1 and π_1 denote the coefficients of the $O(\epsilon)$ terms in (2.24)-(2.27) respectively.

The functions $\Pi_2^{(2)}$, $\Phi_2^{(2)}$, $\Psi_2^{(2)}$ and $\Theta_2^{(2)}$ of η, x_1, σ and M are determined to the required level of approximation by

$$\mathrm{L}_2\Pi_2^{(2)} = M^2\left\{\alpha^2 T F_2^{(2)} - (f'-c)^2\frac{\partial}{\partial\eta}\left[\frac{G_2^{(2)}}{(f'-c)^2}\right]\right\}, \tag{A 5}$$

$$\Phi_2^{(2)} = -\frac{1}{4\alpha^2(f'-c)}\left(M^{-2}\frac{\partial\Pi_2^{(2)}}{\partial\eta} + G_2^{(2)}\right), \tag{A 6}$$

$$\Psi_2^{(2)} = \frac{1}{f'-c}\left(\frac{f'''}{T}\Phi_2^{(2)} - M^{-2}T\Pi_2^{(2)} - \frac{1}{4}F_2^{(2)}\right), \tag{A 7}$$

$$\Theta_2^{(2)} = \frac{1}{f'-c}\left[\frac{T'}{T}\Phi_2^{(2)} + (\gamma-1)(f'-c)T\Pi_2^{(2)} - \frac{1}{4}H_2^{(2)}\right], \tag{A 8}$$

where

$$\mathrm{L}_m \equiv (f'-c)^2\frac{\partial}{\partial\eta}\left[\frac{1}{(f'-c)^2}\frac{\partial}{\partial\eta}\right] - (m\alpha)^2T^2\left[1 - M^2\frac{(f'-c)^2}{T}\right], \tag{A 9}$$

$$F_2^{(2)} \equiv \left[2\Psi_1^2 - \frac{1}{T}\frac{\partial}{\partial\eta}(\Phi_1\Psi_1) + M^{-2}\Theta_1\Pi_1\right]A^{\dagger 2}, \tag{A 10}$$

$$G_2^{(2)} \equiv \frac{1}{2}\left[2\alpha^2\Psi_1\Phi_1 - \frac{\alpha^2}{T}\frac{\partial}{\partial\eta}\left(\Phi_1^2\right) + M^{-2}\frac{\Theta_1}{T}\frac{\partial\Pi_1}{\partial\eta}\right]A^{\dagger 2}, \tag{A 11}$$

$$\begin{aligned} H_2^{(2)} \equiv \Bigg\{&2\Psi_1\Theta_1 - \frac{1}{T}\frac{\partial}{\partial\eta}(\Phi_1\Theta_1) - (\gamma-1)(f'-c)\Pi_1(\Theta_1 + T\Pi_1) \\ &-(\gamma-1)T\left[2\Psi_1\Pi_1 - \frac{1}{T}\frac{\partial}{\partial\eta}(\Phi_1\Pi_1)\right]\Bigg\}A^{\dagger 2}. \end{aligned} \tag{A 12}$$

Similar equations can be obtained for $\Pi_2^{(0)}$, $\Phi_2^{(0)}$, $\Psi_2^{(0)}$ and $\Theta_2^{(0)}$ however, these terms due not contribute to the leading-order behavior of π_2, v_2, u_2 or θ_2 near the critical layer and so can be ignored.

For the purposes of the present analysis, it is only necessary to consider the solutions in the overlap region where $z = O(1)$. In this region, $\Pi_2^{(2)}$ expands like

$$\Pi_2^{(2)} = E_0^{(2)} + \cdots + \sigma\bar{P}_1^{(2)} + \cdots \tag{A 13}$$

where $E_0^{(2)}$ is at most a function of x_1 and $\bar{P}_1^{(2)}$ is the first z-dependent term. Substituting (A 13) along with (2.23), (3.10), (3.11) and (3.23)-(3.25) into (A 5) one finds, after integrating once with respect to z,

$$\frac{\partial \bar{P}_1^{(2)}}{\partial z} = -\frac{4}{9}\bar{\alpha}_0^2\bar{c}_1^2(z-z_c)\left[z_c^2+O(z-z_c)\right]\left(\frac{B_0}{\bar{\alpha}_0^2}A^\dagger\right)^2 \tag{A 14}$$

to lowest order in σ and M as $z \to z_c$. It now follows from (A 6)-(A 8) that

$$\Phi_2^{(2)} = \sigma^{\frac{1}{4}}M^{\frac{3}{2}}\frac{b}{36}\left[z_c^{-1}+O(z-z_c)\right]\left(\frac{B_0}{\bar{\alpha}_0^2}A^\dagger\right)^2, \tag{A 15}$$

$$\Psi_2^{(2)} = \sigma^{-\frac{1}{2}}\left[J_1+O(z-z_c)\right]\left(\frac{B_0}{\bar{\alpha}_0^2}A^\dagger\right)^2, \tag{A 16}$$

and

$$\Theta_2^{(2)} = \sigma^{-\frac{1}{2}}M^2\frac{1}{32}\frac{1}{z-z_c}\left[z_c^3+O(z-z_c)\right]\left(\frac{B_0}{\bar{\alpha}_0^2}A^\dagger\right)^2, \tag{A 17}$$

as $z \to z_c$, where J_1 is an order-one constant.

Appendix B. Higher harmonics in the overlap region

In this appendix, the leading-order approximation to the velocity jump across the critical layer corresponding to the $O(\sigma^{\frac{15}{4}}M^4\epsilon)$ harmonics in (2.24)-(2.27) is determined. Since these harmonics are generated by nonlinear interactions in the critical layer, they take the form

$$u_3 = \sum_{m=2}^{\infty}\mathrm{Re}\Psi_3^{(m)}\hat{a}_3^{(m)}\mathrm{e}^{\mathrm{i}m\bar{X}}, \tag{B 1}$$

$$v_3 = -M^{-\frac{3}{2}}\sum_{m=2}^{\infty}\mathrm{Re}\mathrm{i}m\bar{\alpha}\Phi_3^{(m)}\hat{a}_3^{(m)}\mathrm{e}^{\mathrm{i}m\bar{X}}, \tag{B 2}$$

$$\theta_3 = \sum_{m=2}^{\infty}\mathrm{Re}\Theta_3^{(m)}\hat{a}_3^{(m)}\mathrm{e}^{\mathrm{i}m\bar{X}}, \tag{B 3}$$

and

$$\pi_3 = \sum_{m=2}^{\infty}\mathrm{Re}\Pi_3^{(m)}\hat{a}_3^{(m)}\mathrm{e}^{\mathrm{i}m\bar{X}}, \tag{B 4}$$

where the scaled harmonic amplitudes $\hat{a}_3^{(m)}(x_1)$ are determined by the nonlinear flow within the critical layer and the functions $\Psi_3^{(m)}$, $\Phi_3^{(m)}$, $\Theta_3^{(m)}$ and $\Pi_3^{(m)}$ of η, x_1, σ and M are determined by the following linear equations outside the critical layer,

$$\mathrm{L}_m \Pi_3^{(m)} = 0, \tag{B 5}$$

$$\Phi_3^{(m)} = -\frac{M^{-2}}{m^2\alpha^2\,(f'-c)}\frac{\partial}{\partial\eta}\Pi_3^{(m)}, \tag{B 6}$$

$$\Psi_3^{(m)} = \frac{1}{f'-c}\left(\frac{f''}{T}\Phi_3^{(m)} - M^{-2}T\Pi_3^{(m)}\right), \tag{B 7}$$

and

$$\Theta_3^{(m)} = \frac{1}{f'-c}\left[\frac{T'}{T}\Phi_3^{(m)} + (\gamma-1)\,(f'-c)\,T\Pi_3^{(m)}\right]. \tag{B 8}$$

These functions satisfy the usual homogenous boundary conditions at the wall and decay exponentially as $\eta \to \infty$. However, they are, in general, discontinuous across the critical layer.

It is only necessary to consider the solutions in the overlap region where $z = O(1)$. In order for the solutions in this region to match with those in the wall and temperature adjustment layers, $\Pi_3^{(m)}$ must expand like

$$\Pi_3^{(m)} = 1 + \cdots + \sigma^{\frac{3}{2}}\bar{P}_1^{(m)-} + \cdots, \tag{B 9}$$

for $z < z_c$, and

$$\Pi_3^{(m)} = 1 + \cdots + \sigma^{-\frac{1}{4}}M^{-2}\bar{P}_1^{(m)+} + \cdots, \tag{B 10}$$

for $z > z_c$, where $\bar{P}_1^{(m)\pm}$ is the first z-dependent term. Equations (B 9) and (B 10) imply that the pressure fluctuations are constant across the critical layer to $O(\sigma^{\frac{15}{4}}M^4\epsilon)$ (a fact that can be deduced from the transverse component of the momentum equation in the critical layer), but that the pressure gradient is discontinuous at $O(\sigma^{\frac{7}{2}}M^2\epsilon)$. Substituting (B 10) along with

(2.23), (3.10), (3.11) and (3.23)-(3.25) into (B 5) one finds, after integrating once with respect to z,

$$\frac{\partial}{\partial z}\bar{P}_1^{(m)+} = -m\bar{\alpha}_0\frac{16}{z_c^2}(z-z_c)^2 + \cdots \tag{B 11}$$

as $z \to z_c$ from above. It now follows from (B 6)-(B 8) that

$$\Phi_3^{(m)} = \sigma^{-1}M^{-\frac{1}{2}}\frac{1}{m\bar{\alpha}_0\bar{c}_1}\frac{4}{z_c}(z-z_c) + \cdots, \tag{B 12}$$

$$\Psi_3^{(m)} = \sigma^{-\frac{7}{4}}M^{-2}\frac{1}{m\bar{\alpha}_0\bar{c}_1^2}\frac{b}{9z_c} + \cdots, \tag{B 13}$$

and

$$\Theta_3^{(m)} = -\sigma^{-\frac{7}{4}}\frac{1}{m\bar{\alpha}_0\bar{c}_1^2}\frac{4}{z_c} + \cdots, \tag{B 14}$$

as $z \to z_c$ from above. It can be shown that the solution for $\Psi_3^{(m)}$ is $o(\sigma^{-\frac{7}{4}}M^{-2})$ as $z \to z_c$ from below, therefore the leading-order approximation to the velocity jump across the critical layer associated with the higher harmonics is given as

$$\Delta u_3 \equiv u_3(z_c^+) - u_3(z_c^-) = \sigma^{-\frac{7}{4}}M^{-2}\sum_{m=2}^{\infty}\mathrm{Re}\frac{1}{m\bar{\alpha}_0\bar{c}_1^2}\frac{b}{9z_c}\hat{a}_3^{(m)}\mathrm{e}^{\mathrm{i}m\bar{X}} + \cdots. \tag{B 15}$$

REFERENCES

BLACKABY, N. D., COWLEY, S. J. & HALL, P. 1992 On the instability of hypersonic flow past a flat plate. Submitted to *J. Fluid Mech.*

BUSH, W. B. & CROSS, A. K. 1967 Hypersonic weak-interaction similarity solutions for flow past a flat plate. *J. Fluid Mech.* **29**, 349-359.

COWLEY, S. J. & HALL, P. 1990 On the instability of hypersonic flow past a wedge. *J. Fluid Mech.* **214**, 17-42.

FREEMAN, N. C. & LAM, S. H. 1959 On the Mach number independence principle for a hypersonic boundary layer. *Princeton University Report* 471.

FU, Y. B., HALL, P. & BLACKABY, N. D. 1990 On the Görtler instability in hypersonic flows: Sutherland law fluids and real gas effects. *ICASE Report No.* 90-85

GAJJAR, J. S. B. & COLE, J. W. 1989 Upper branch stability of compressible boundary layer flows. *Theor. Comp. Fluid Dyn.* **1**, 105-123.

GOLDSTEIN, M. E., DURBIN, P. A. & LEIB, S. J. 1987 Roll-up of vorticity in adverse-pressure-gradient boundary layers. *J. Fluid Mech.* **183**, 325-342.

GOLDSTEIN, M. E. & HULTGREN, L. S. 1988 Nonlinear spatial evolution of an externally excited instability wave in a free shear layer. *J. Fluid Mech.* **197**, 295-330.

GOLDSTEIN, M. E. & LEIB, S. J. 1988 Nonlinear roll-up of externally excited free shear layers. *J. Fluid Mech.* **191**, 481-515.

GOLDSTEIN, M. E. & LEIB, S. J. 1989 Nonlinear evolution of oblique waves on compressible shear layers. *J. Fluid Mech.* **207**, 73-96.

GOLDSTEIN, M. E. & WUNDROW, D. W. 1990 Spatial evolution of nonlinear acoustic mode instabilities on hypersonic boundary layers. *J. Fluid Mech.* **219**, 585-607.

GRUBIN, S. E. & TRIGUB, V. N. 1992a The asymptotic theory of a hypersonic boundary layer stability. Submitted to *J. Fluid Mech.*

GRUBIN, S. E. & TRIGUB, V. N. 1992b The long-wave limit in the asymptotic theory of a hypersonic boundary layer stability. Submitted to *J. Fluid Mech.*

LEES, L. & LIN, C. C. 1946 Investigation of the stability of the laminar boundary layer in a compressible fluid. *NACA Tech. Note No.* 115

LEIB, S. J. 1991 Nonlinear evolution of subsonic and supersonic disturbances on a compressible free shear layer. *J. Fluid Mech.* **224**, 551-578.

MACK, L. M. 1984 Boundary-layer linear stability theory. In *Special Course on Stability and Transition of Laminar Flow. AGARD Report No.* 709.

MACK, L. M. 1987 Review of linear compressible stability theory. In *Stability of Time Dependent and Spatially Varying Flows*, eds. D. L. Dwoyer & M. Y. Hussaini. Springer-Verlag.

RESHOTKO, E. 1960 Stability of the compressible laminar boundary layer. *GALCIT Memo* 52. Calif. Inst. of Technology, Pasadena, CA.

SMITH, F. T. & BROWN, S. N. 1990 The inviscid instability of a Blasius boundary layer at large values of the Mach number. *J. Fluid Mech.* **219**, 499-518.

STEWARTSON, K. 1964 *Theory of Laminar Boundary Layers in Compressible Fluids.* Oxford University Press.

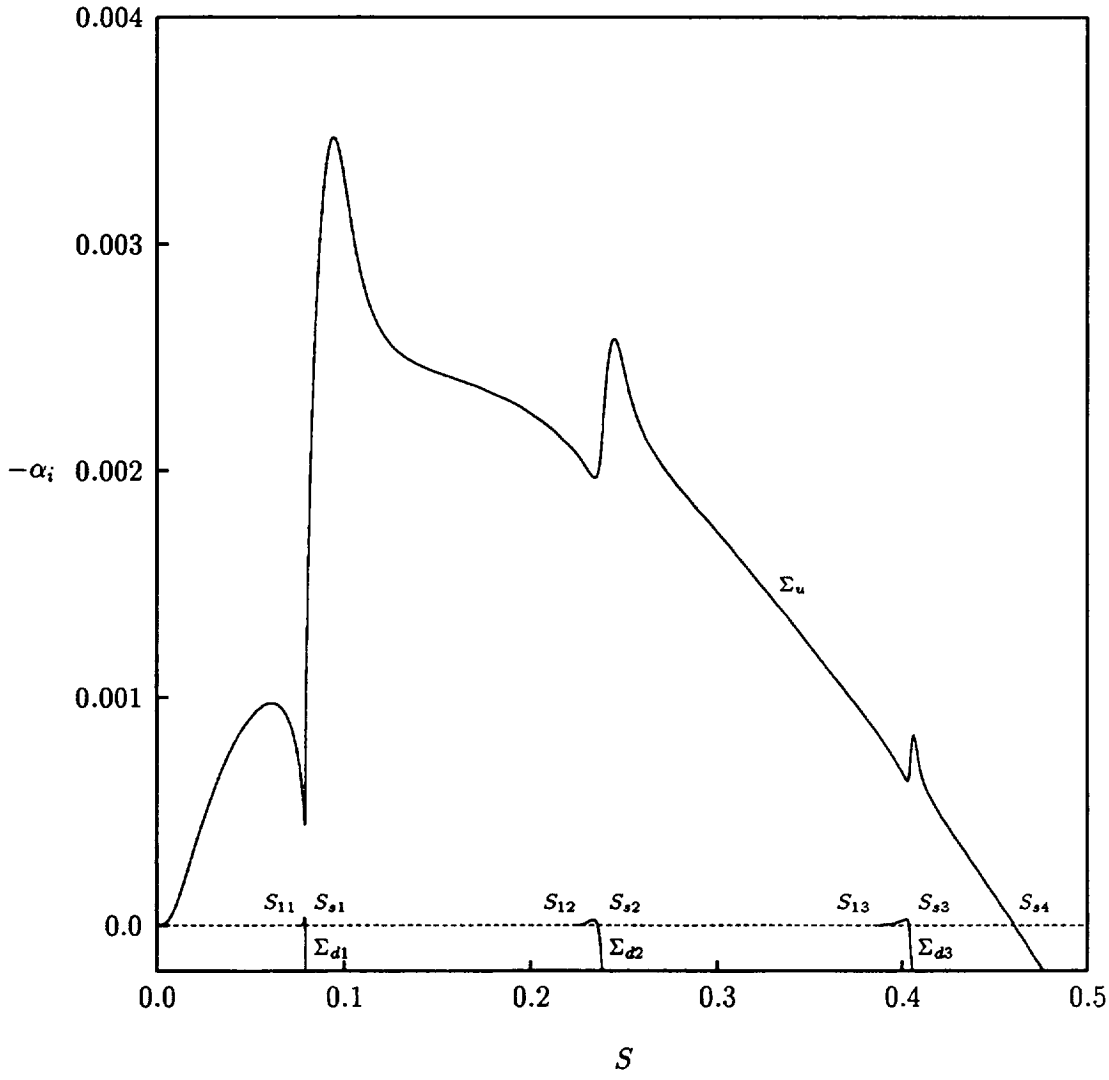

FIGURE 1. Growth rate vs. frequency for an insulated plate at $M = 10$.

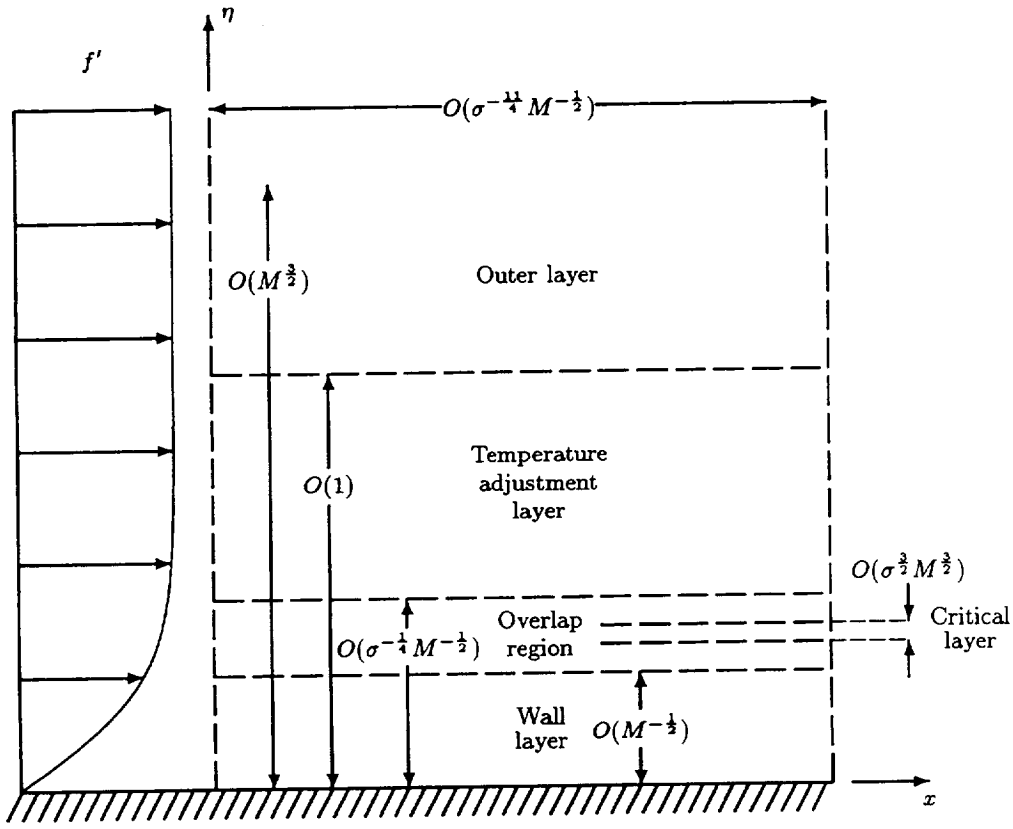

FIGURE 2. Asymptotic structure of the large-Mach-number solution in the Dorodnitsyn-Howarth variable.

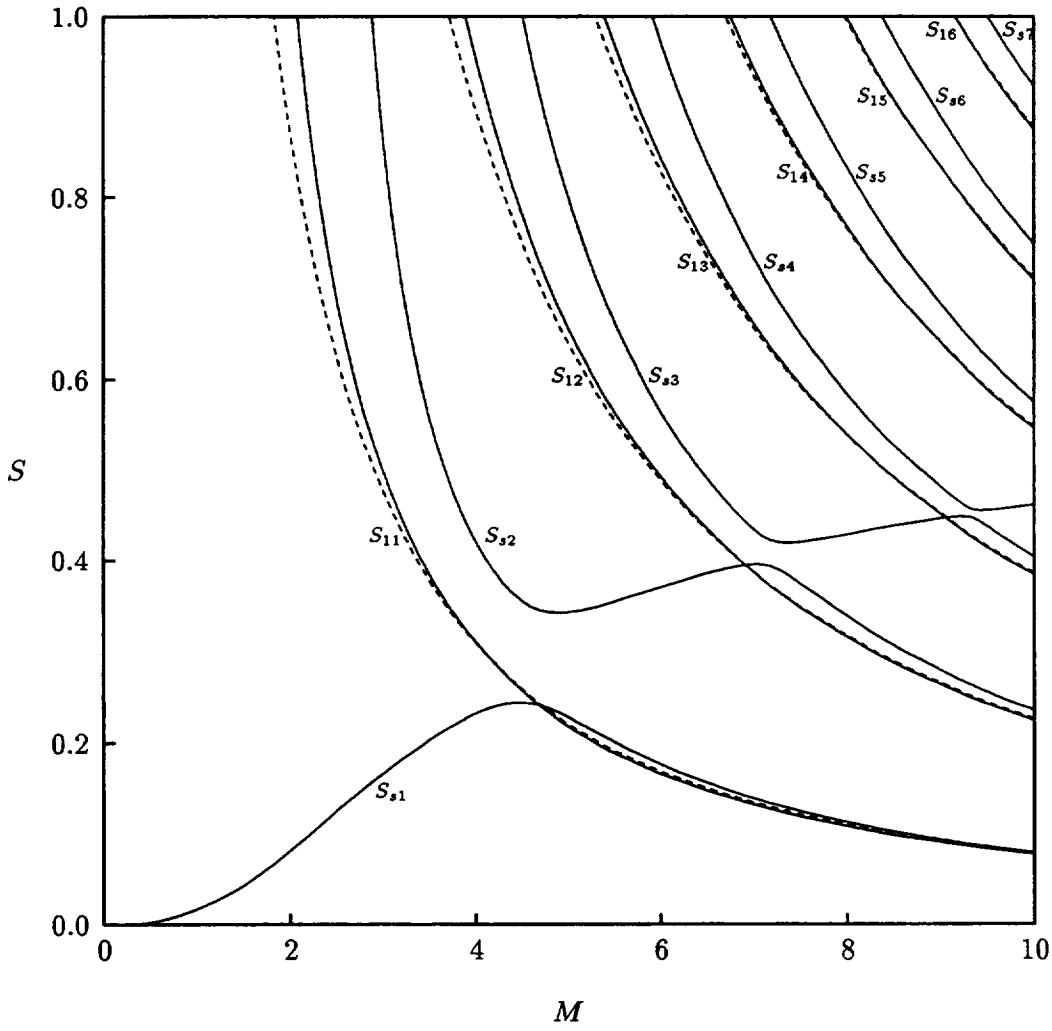

FIGURE 3. Neutral frequencies vs. Mach number for an insulated plate. Solid lines, exact solution; dashed lines, asymptotic solution.

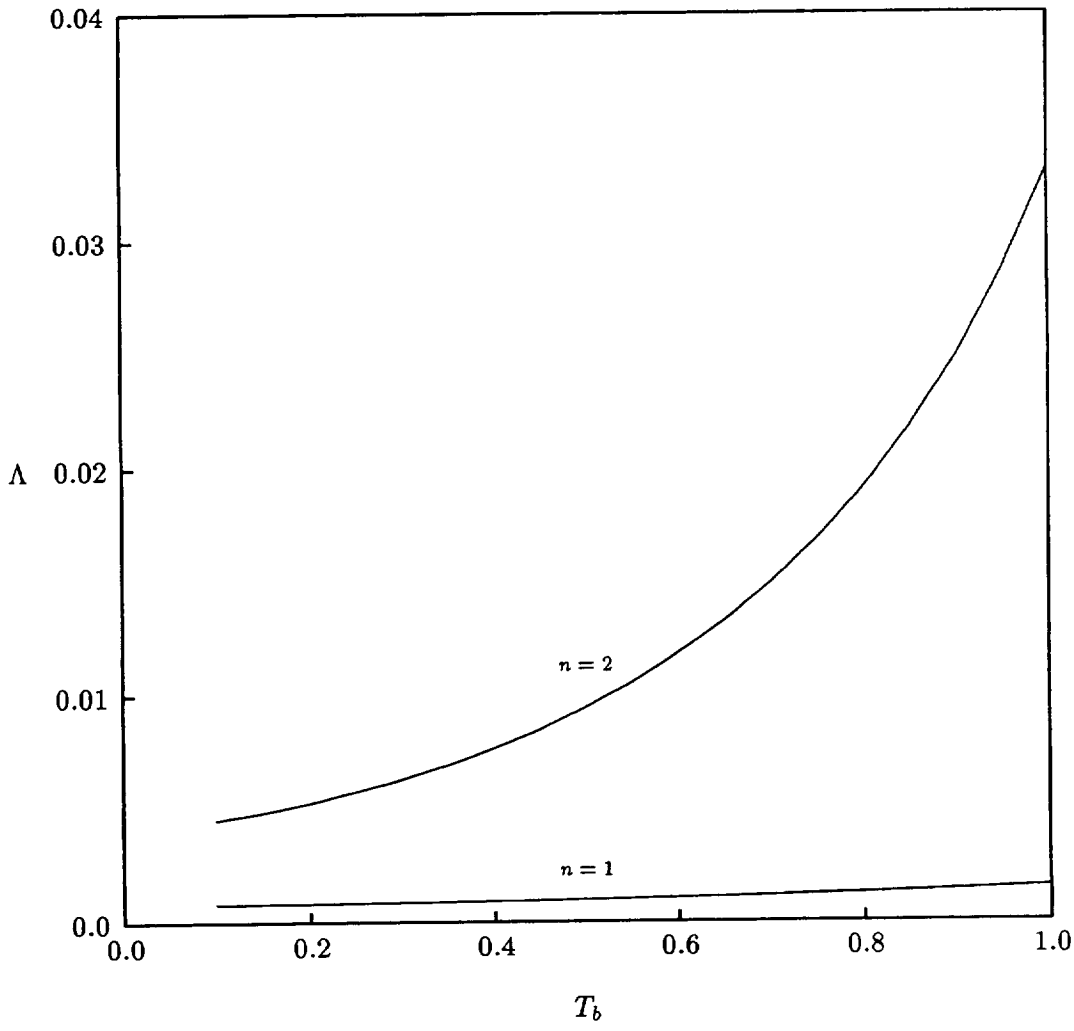

FIGURE 4. Λ vs. T_b for the first two values of $\bar{\alpha}_0$.

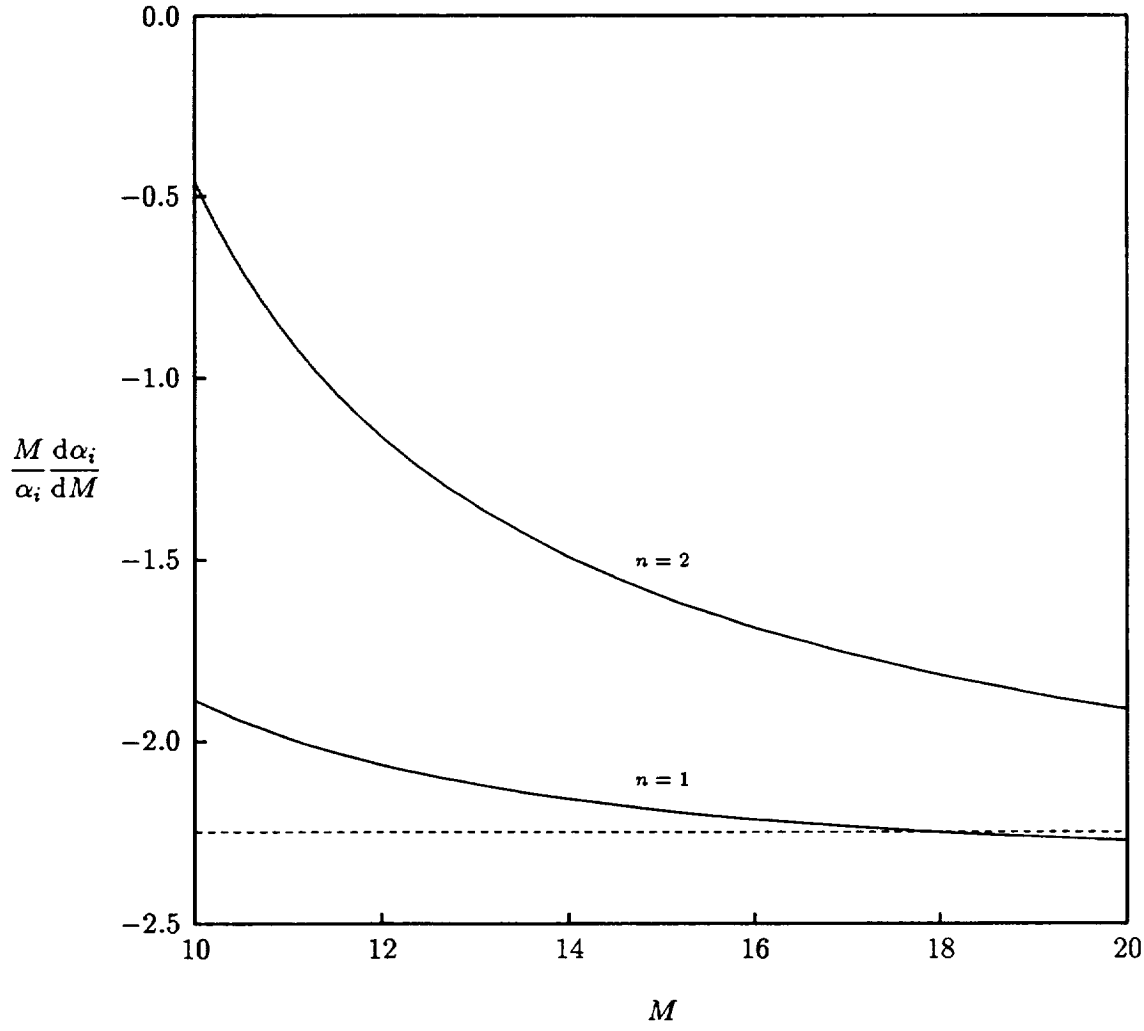

FIGURE 5. Growth rate scaling vs. Mach number for an insulated plate. Solid lines, exact solutions for $\lambda = 0.1$; Dashed line, asymptote from hypersonic theory.

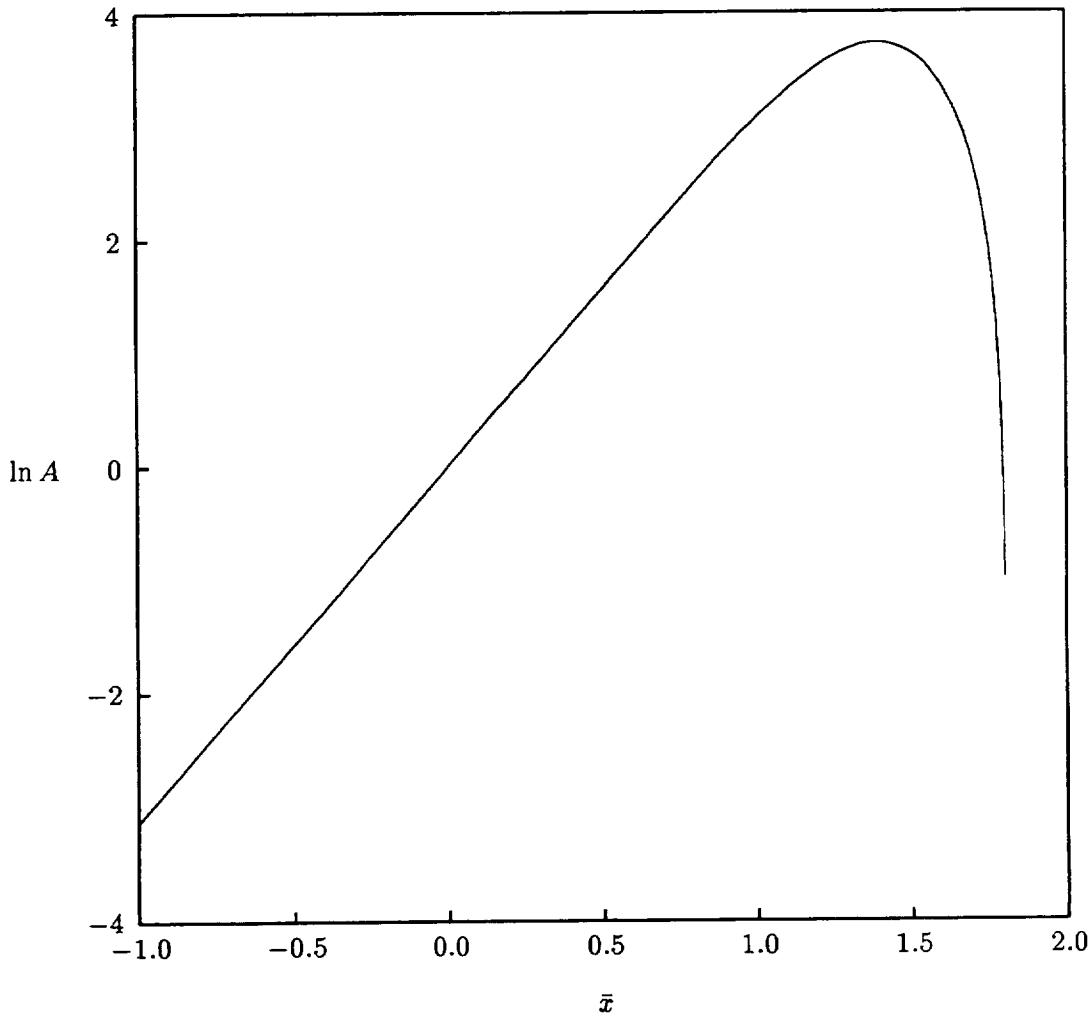

FIGURE 6. Scaled instability-wave amplitude vs. long streamwise distance.

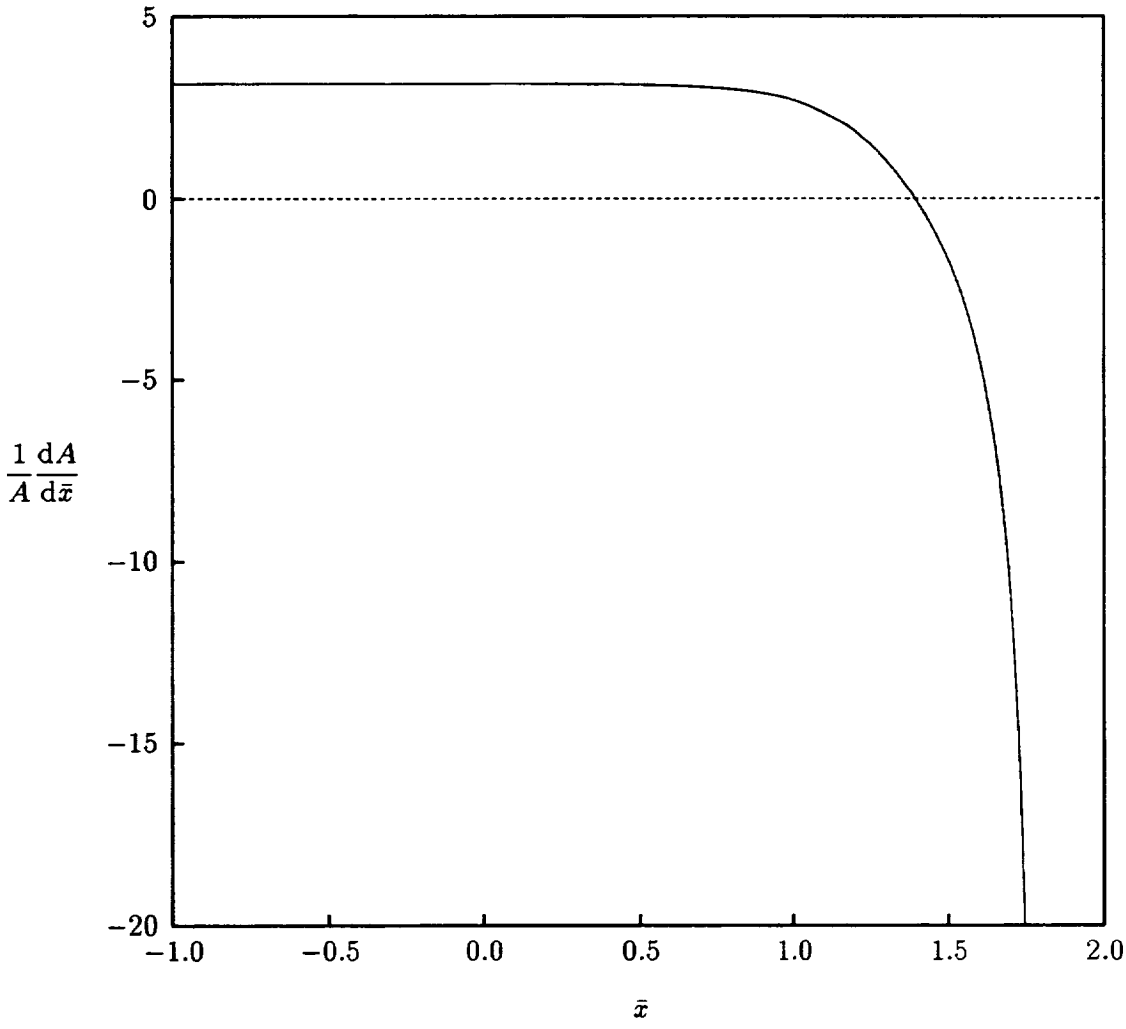

FIGURE 7. Scaled instability-wave growth rate vs. long streamwise distance.

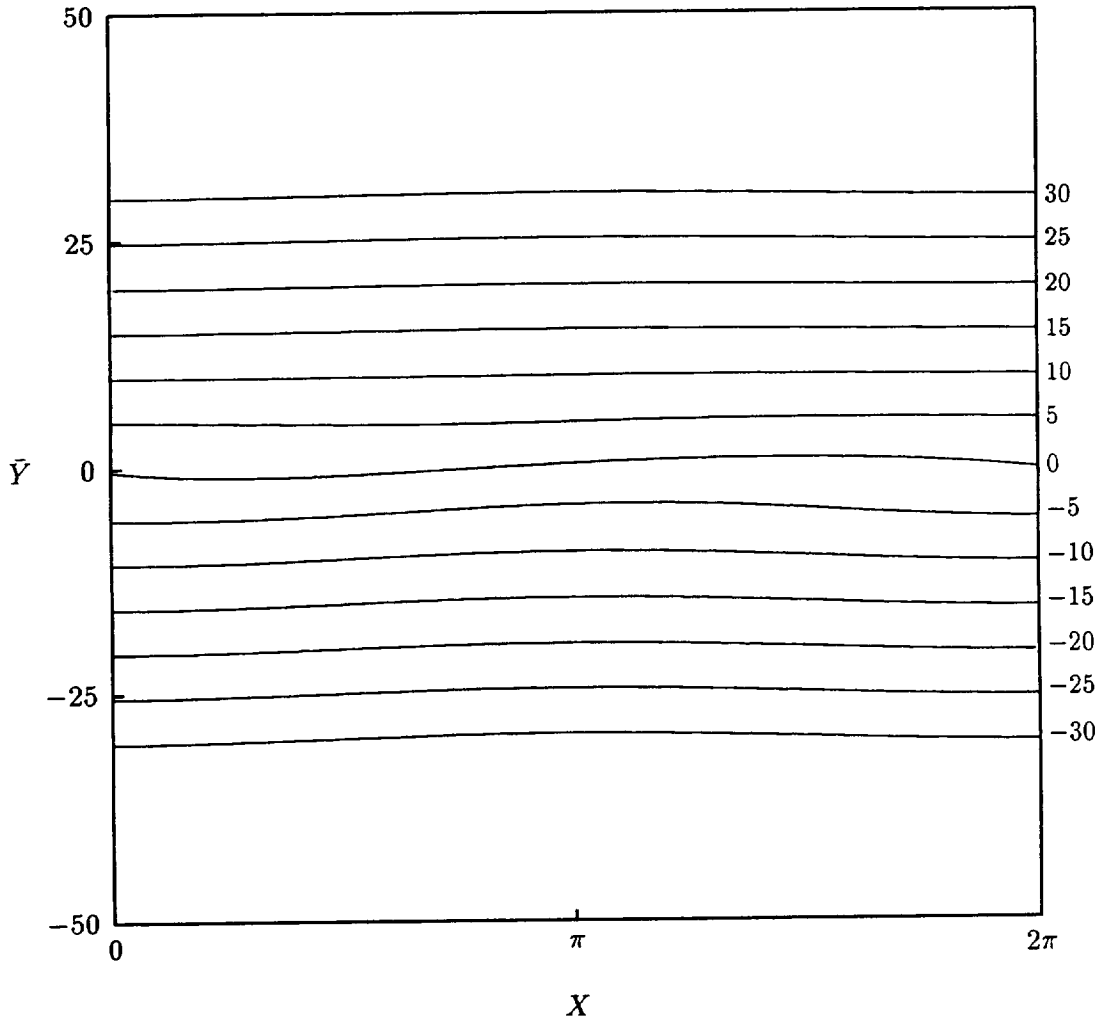

FIGURE 8(a). Vorticity contours in the $(X, \bar{Y})$-plane at $\bar{x} = 0$.

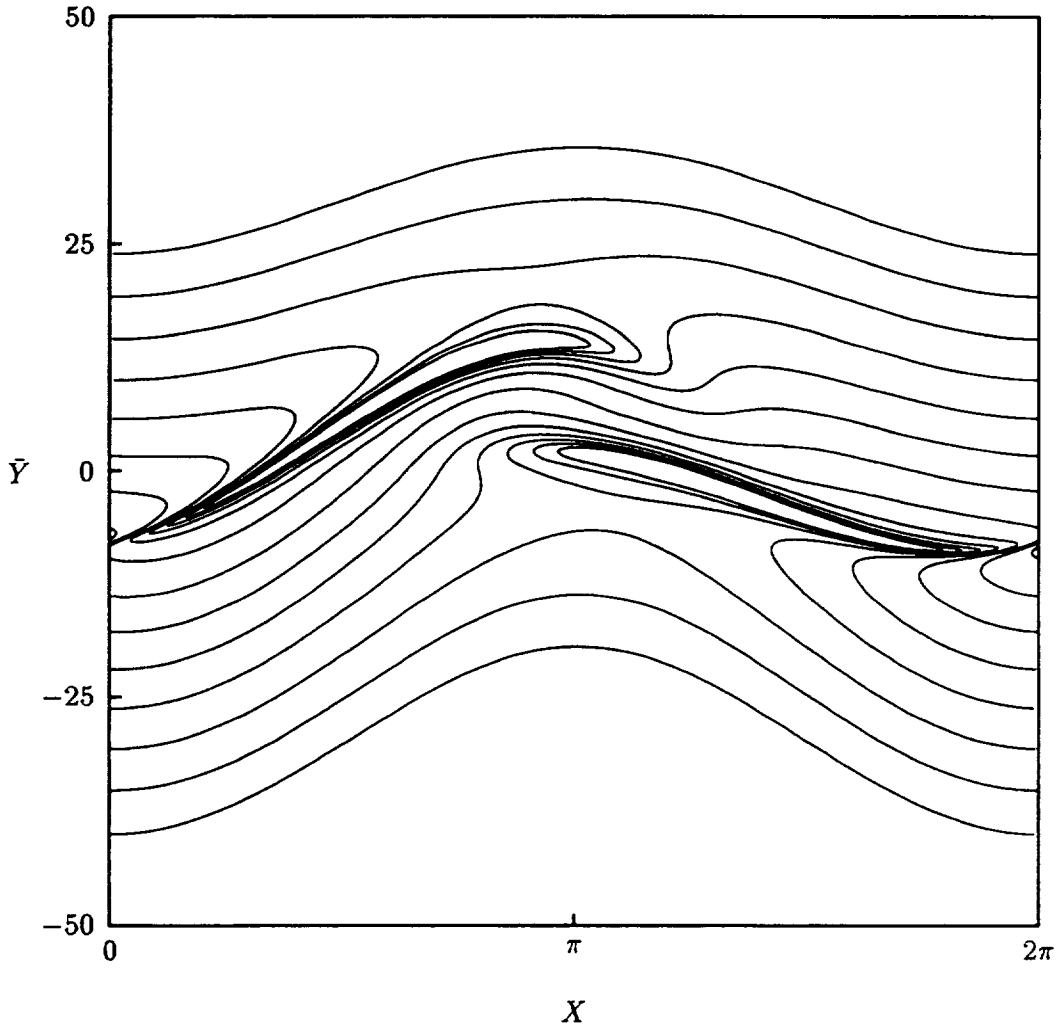

FIGURE 8(b). Vorticity contours in the $(X, \bar{Y})$-plane at $\bar{x} = 1$.

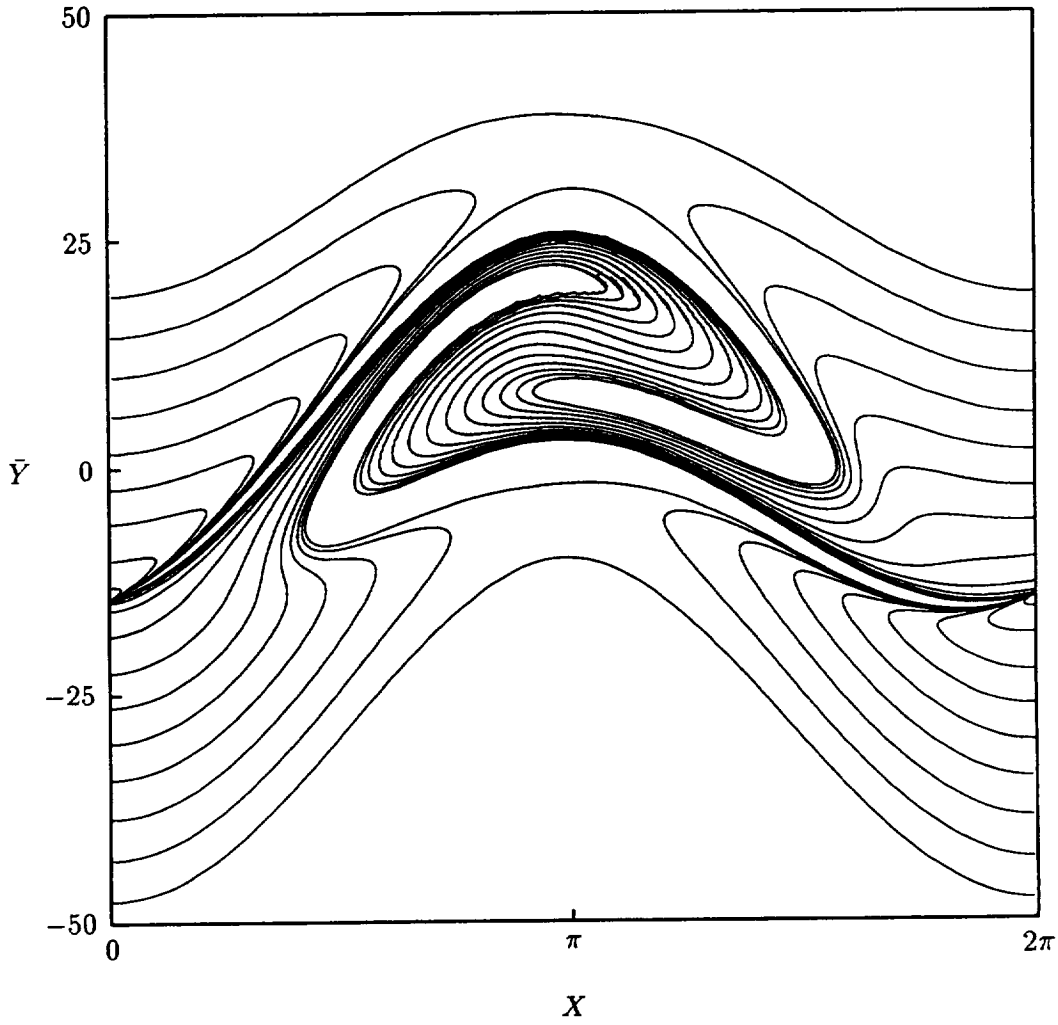

FIGURE 8(c). Vorticity contours in the $(X, \bar{Y})$-plane at $\bar{x} = 1.5$.

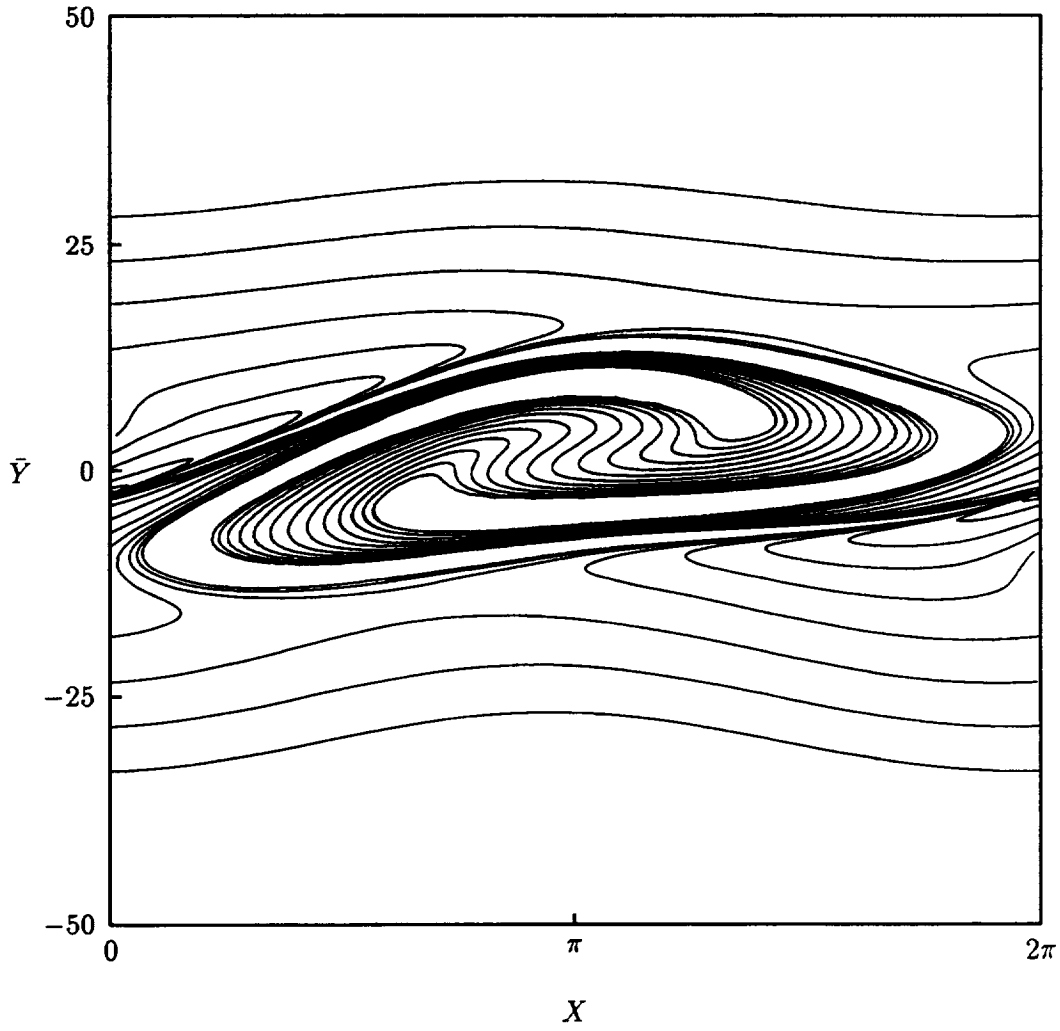

FIGURE 8(d). Vorticity contours in the $(X, \bar{Y})$-plane at $\bar{x} = 1.75$.

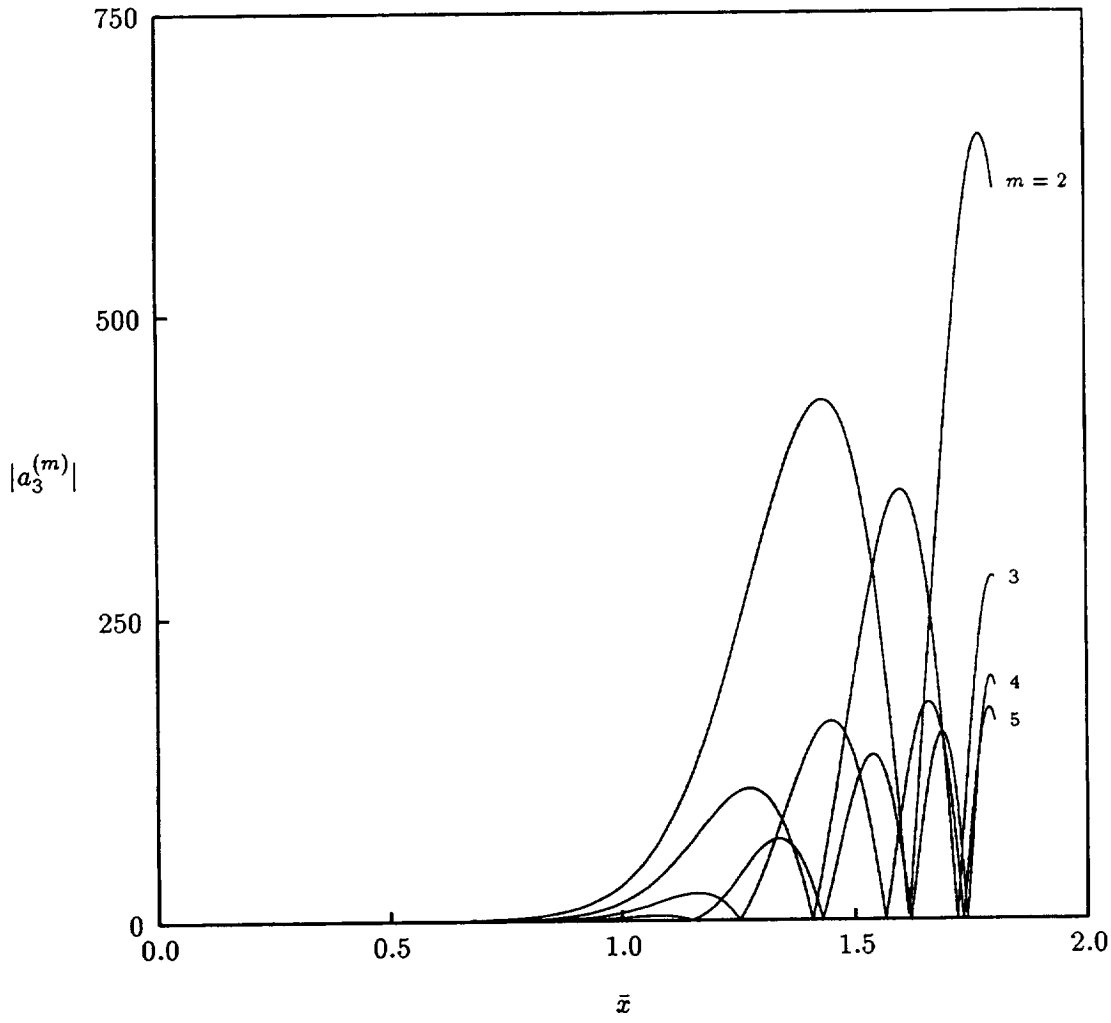

FIGURE 9. Scaled harmonic amplitudes vs. long streamwise distance.

REPORT DOCUMENTATION PAGE

Form Approved
OMB No. 0704-0188

1. AGENCY USE ONLY (*Leave blank*)	2. REPORT DATE	3. REPORT TYPE AND DATES COVERED
	May 1996	Final Contractor Report

4. TITLE AND SUBTITLE

Nonlinear Spatial Evolution of Inviscid Instabilities on Hypersonic Boundary Layers

5. FUNDING NUMBERS

WU-505-90-53
C-NAS3-27186

6. AUTHOR(S)

David W. Wundrow

7. PERFORMING ORGANIZATION NAME(S) AND ADDRESS(ES)

NYMA, Inc.
2001 Aerospace Parkway
Brook Park, Ohio 44142

8. PERFORMING ORGANIZATION REPORT NUMBER

E-10223

9. SPONSORING/MONITORING AGENCY NAME(S) AND ADDRESS(ES)

National Aeronautics and Space Administration
Lewis Research Center
Cleveland, Ohio 44135-3191

10. SPONSORING/MONITORING AGENCY REPORT NUMBER

NASA CR-198477

11. SUPPLEMENTARY NOTES

Project Manager, Marvin E. Goldstein, Lewis Research Academy, NASA Lewis Research Center, organization code 0130, (216) 433-5825.

12a. DISTRIBUTION/AVAILABILITY STATEMENT

Unclassified - Unlimited
Subject Categories 01 and 34

This publication is available from the NASA Center for AeroSpace Information, (301) 621-0390.

12b. DISTRIBUTION CODE

13. ABSTRACT (*Maximum 200 words*)

The spatial development of an initially linear vorticity-mode instability on a compressible flat-plate boundary layer is considered. The analysis is done in the framework of the hypersonic limit where the free-stream Mach number $M \to \infty$. Nonlinearity is shown to become important locally, in a thin critical layer, when σ, the deviation of the phase speed from unity, becomes $o(M^{-8/7})$ and the magnitude of the pressure fluctuations becomes $O(\sigma^{5/2}M^2)$. The unsteady flow outside the critical layer takes the form of a linear instability wave but with its amplitude completely determined by the nonlinear flow within the critical layer. The coupled set of equations which govern the critical-layer dynamics reflect a balance between spatial-evolution, (linear and nonlinear) convection and nonlinear vorticity-generation terms. The numerical solution to these equations shows that nonlinear effects produce a dramatic reduction in the instability-wave amplitude.

14. SUBJECT TERMS	15. NUMBER OF PAGES
Hypersonic; Stability; Boundary layer	53
	16. PRICE CODE: A04

17. SECURITY CLASSIFICATION OF REPORT	18. SECURITY CLASSIFICATION OF THIS PAGE	19. SECURITY CLASSIFICATION OF ABSTRACT	20. LIMITATION OF ABSTRACT
Unclassified	Unclassified	Unclassified	

National Aeronautics and
Space Administration
Lewis Research Center
21000 Brookpark Rd.
Cleveland, OH 44135-3191